PERVIOUS CONCRETE WITH TITANIUM DIOXIDE AS A PHOTOCATALYST COMPOUND FOR A GREENER URBAN ROAD ENVIRONMENT

By

MARIA CHRISTINA BURTON

A thesis submitted in partial fulfillment of the requirements for the degree of

MASTER OF SCIENCE IN CIVIL ENGINEERING

WASHINGTON STATE UNIVERSITY
Department of Civil and Environmental Engineering

DECEMBER 2011

To the Faculty of Washington State University:

The members of the Committee appointed to examine the thesis of MARIA CHRISTINA BURTON find it satisfactory and recommend that it be accepted.

Shihui Shen, Ph.D., Chair

Liv Haselbach, Ph.D.

Bertram T. Jobson, Ph.D.

ACKNOWLEDGMENT

The writer gratefully acknowledges guidance from Dr. Shihui Shen, Dr. Liv Haselbach, and Dr. Bertram T. Jobson, as well as assistance on experiments from fellow colleagues. Acknowledgment would also like to be given to the Transportation Northwest (TransNow) through the US DOT for funding support and Washington State University Capital Planning and Development, along with donations from Cristal Global and Pureti, Holcim Inc., and Atlas Sand & Rock for titanium dioxide, cement, and aggregates respectively.

PERVIOUS CONCRETE WITH TITANIUM DIOXIDE AS A PHOTOCATALYST COMPOUND FOR A GREENER URBAN ROAD ENVIRONMENT

Abstract

by Maria Christina Burton, M.S.
Washington State University
December 2011

Chair: Shihui Shen

The United States is facing the problem of controlling air pollution from vehicle emissions, especially in growing urban areas. The photocatalyst, titanium dioxide (TiO_2), activates with ultraviolet (UV) radiation to oxidize air pollutants, such as nitrogen oxides (NO_x) and volatile organic compounds (VOCs). Applying the photocatalytic effect of TiO_2 onto pervious concrete pavement to remove pollutants from the air appeared to be a promising alternative to remove pollutants from street level. This study compared different methods to apply TiO_2 onto the surface of pervious concrete and measured the effectiveness of the surface coating materials in removing air pollutants, maintaining infiltration properties, and withstanding environmental weathering. A brief analysis on the material cost of each application method is also presented.

High pollutant reductions were seen with a driveway protector mix, a commercial water-based TiO_2 preparation, TiO_2 in water, a cement-water slurry with low cement concentration, and the commercial PURETI coating. It was found that nitric oxide (NO) was efficiently removed

with each of these treatments, while VOCs displayed more variability in removal efficiency. When pervious concrete was compared to traditional concrete, pervious concrete showed higher NO reductions. Most coating methods maintained an acceptable level of infiltration rate for pervious concrete pavements. The driveway protector mix had the highest resistance against freeze-thaw testing with deicing chemical and environmental weathering.

The evaluated coating methods are recommended for different applications. The driveway protector mix resists environmental weathering well and can be used for highway shoulders and locations where weathering could be a concern. The transparent color of the commercial water-based TiO_2 could be used for aesthetic reasons. The cement aggregate mixes could be used as a thin pervious concrete overlay to at the same time address minor pavement surface distress. The PURETI treatment is a cost-effective alternative, where the surface abrasion is low. More studies need to be done to optimize each application method and confirm their resistance against live traffic and environmental damage. Fundamental research should also be conducted to investigate the sequential chemical reactions during the complex photocatalytic process to substantiate the environmental benefits of the photocatalytic materials in the field.

TABLE OF CONTENTS

LIST OF TABLES

LIST OF FIGURES

Dedication

This thesis is dedicated to my mother and father

who provided both emotional and financial support.

CHAPTER ONE

INTRODUCTION

1.1 INTRODUCTION

The demand for pavement increases as cities grow. Though pavement may be beneficial for transportation, it can have negative impacts on the environment. Most pavements used are impermeable, resulting in more surface water runoff and less groundwater recharge. Effort has been put into reducing the impermeable surfaces of buildings by placing "green" roofs on them, but there are still parking lots, sidewalks, and miles of roadways that stretch throughout cities. Implementing permeable pavements whenever possible will have significant benefit to stormwater management (Brown, 2003; Montes & Haselbach, 2006), reduced heat island effect (Yang & Jiang, 2003; Haselbach, 2009), and reduced pavement noise due to traffic (Yang & Jiang, 2003; Olek et al., 2003), hence, produce a more sustainable transportation environment in urban cities.

Emissions from vehicle traffic cause air pollutant problems throughout the world. There have been many attempts to reduce emissions, from encouragement of carpooling and public transportation to redesigning the vehicles themselves. However, there are still emissions polluting the air to a significant degree. The U.K. is currently facing a fine of $500 million for London exceeding the PM_{10} particle pollution limits more than 35 times for the entire year (Morales, 2011). The PM_{10} particles are mainly from vehicles, factories, and construction. A London study found that a primary school near a high traffic street left the school children

vulnerable to significant air pollution exposure (Moussiopoulos et al., 2007). The London study also confirmed the benefit of applying photocatalytic coating to materials on a large scale to reduce air pollution in urban areas.

The photocatalyst, titanium dioxide (TiO_2), is a naturally occurring compound that can decompose gaseous pollutants with the presence of sunlight. Applying TiO_2 to pavement can help remove emission pollutants right next to the source, near the vehicles that drive on the pavement itself. However, surface coatings to traditional pavements may lose their effectiveness due to surface wear. When TiO_2 is applied to pervious pavement, this provides two sustainable benefits in one material; air will be purified on sunny days, and water will be infiltrated on rainy days, in addition to having a rougher surface, which may retain more TiO_2. With this innovative idea, this paper aims to identify the effectiveness of applying TiO_2 to the surface of pervious concrete pavement to produce a greener urban road environment. Several coating methods were compared for their influence on permeability, pollutant removal effectiveness, and their resistance to extreme environmental conditions.

1.2 PROBLEM STATEMENT

Air and water are vital to the existence of life on Earth. With their highly trafficked transportation systems, cities produce a significant amount of air pollution due to vehicle emissions, and they reduce the amount of groundwater recharge due to the extensive use of impermeable pavements. Impermeable pavements also contribute to the urban heat island effect. These problems are not natural, and the larger the cities grow, the more they will disrupt the quality of life on Earth by contributing more to these problems. It is important to keep the air

clean and water charged to acceptable natural levels so that the Earth can stay sustained for future generations without becoming impoverished.

1.3 OBJECTIVES

The objective of this study is to evaluate the effectiveness of TiO_2 treated pervious concrete by comparing different TiO_2 application methods for their capability of pollutant reduction, maintaining the infiltrating characteristic of the pervious concrete, and withstanding environmental damage. TiO_2 distribution for each application method was analyzed using a scanning electron microscope (SEM). A laboratory environmental setup was used to evaluate the pollutant removal efficiency due to the photocatalytic effect of the TiO_2. Because a major focus of this application is in the transportation environment, three different gaseous pollutants that are present in automobile exhaust were tested: toluene, trimethylbenzene, and NO. Infiltration was tested to ensure the surface treatments did not reduce the infiltrating characteristic of the pervious concrete. The material's durability against environmental damage was evaluated under freeze-thaw condition with de-icing agent and natural weathering outside.

1.4 ORGANIZATION OF THESIS

This thesis is organized into five chapters. The first chapter introduces the motivation of this research. The second chapter reviews previous related research. The third chapter explains the testing procedures that were followed, including sample preparation and porosity and infiltration testing. The fourth chapter evaluates and compares the results of the different sample types based on infiltration testing, environmental chamber testing, image analysis under a

scanning electron microscope, weathering durability, and an analysis on the material costs to employ each sample type. The fifth and final chapter concludes this research with recommendations based on the data that was obtained.

CHAPTER TWO

LITERATURE REVIEW

This chapter consists of three parts. The first part reviews the existing applications of titanium dioxide in engineering practice. It reviews the photocatalytic effect of TiO_2, the hydrophilic effect of TiO_2, applications utilizing the photocatalytic and hydrophilic effect of TiO_2, and the cost and maintenance to use TiO_2 for applications. The second part reviews the existing applications of pervious concrete in engineering practice. It reviews the benefits of installing pervious concrete pavement, pavement applications utilizing the benefits of pervious concrete, and the cost and maintenance to use pervious concrete for applications. The third part reviews the possible benefits for installing pervious concrete pavement treated with TiO_2.

2.1 TITANIUM DIOXIDE

Titanium dioxide is a naturally occurring compound and is used in toothpaste, sunscreen, paint, plastics, cosmetics, and other products. Because it is white, harmless, and inexpensive, TiO_2 powders were used for white pigments in ancient times (Hashimoto, Irie, & Fujishima, 2005). It is used in sunscreen because it can absorb UV light without being consumed in the reaction (Katzman, 2006).

2.1.1 Phtocatalytic Effect of TiO_2

In the sunlight, TiO_2 can have a photocatalytic effect, in which it turns into a "photo-bleach" and will degrade fabrics and paint when sunlight is present (Hashimoto et al., 2005). A

photocatalyst is “a material that uses solar energy to accelerate chemical reactions without being consumed or depleted in the process” (Chusid, 2006). Photocatalysis of TiO_2 powders started developing in industrial technology in the 1980s (Hashimoto et al., 2005). Heterogeneous photocatalytic reactions have been studied for more than fifty years, as of 2009 (Puzenat, 2009). Researchers in Europe and Japan have been studying photocatalytic compounds and how they can reduce pollution for over four years, as of 2006 (Katzman, 2006).

In the sunlight, TiO_2 is activated by ultraviolet (UV) radiation ($\lambda < 390$ nm) to oxidize air pollutants, such as nitrogen oxides (NO_x) and volatile organic compounds (VOCs), into other inorganic compounds. In a photocatalytic reaction with TiO_2, no chemical reactants are used. The TiO_2 does not get consumed in the reaction; so it can theoretically be used indefinitely. TiO_2 photocatalysis can be performed even in weak UV light (Hashimoto et al., 2005). TiO_2 (anatase) has a wide band gap, thus only ultraviolet light with a wavelength below 387 nm is absorbed (Fernandez-Rodriguez et al., 2009; Hong et al., 2005).

Photocatalysts activated by UV lights will decompose organic materials like components of dirt (soot, grime, oil, and particulates), biological organisms (mold, algae, bacteria, and allergens), airborne pollutants (VOC, tobacco smoke, NO_x, and SO_x), and chemicals that cause odors (Chusid, 2006). Most inorganic pollutants, like rust stains, are not catalyzed (Chusid, 2006). The decomposition products are oxygen, carbon dioxide, water, sulfate, nitrate, and other inorganic molecules.

There are many commercial products that use photocatalytic reactions to make them self-cleaning materials. Some successful examples are glasses, tiles, and concrete (Puzenat, 2009). Titanium dioxide is used in concrete for buildings and ceramics for tiles, but only the part at the surface can be activated (Puzenat, 2009). These products can self-clean and reduce NOx in the

atmosphere. These applications are largely developed in Japan by Toto company and also in Europe with the product, TX Active, from Italcementi.

The Italian company, Italcementi, developed a type of cement with titanium dioxide on the surface called TX Active ("New kind of cement absorbs pollution," 2006). Tests on a road have shown it to reduce the nitrogen dioxide and carbon monoxide by up to 65 percent. The photocatalysis process of the titanium dioxide worked best in bright sunlight. TX Active cement has been used on buildings such as Paris' Charles de Gaulle Airport, Rome's Dives in Misericordia church, and Bordeaux's Hotel de Police.

Photocatalytic concrete is starting to be used more in architectural and civil engineering projects in Europe and Asia as a self-cleaning material. Some benefits of photocatalytic concrete are that it decomposes chemicals that contribute to soiling and air pollution, it keeps the concrete cleaner, and it reflects much of the sun's heat and reduces heat gain because of its white color (Chusid, 2006). Italcementi's TX Active photocatalytic cements that self-clean and depollute air are now available in North America (Chusid, 2006). The precast concrete Jubilee Church in Rome, built in 2003, has white concrete elements that are at 85 feet high. To keep it clean in the polluted neighborhood that it is located in, Italcementi's TX Active photocatalytic cement was used (Chusid, 2006).

TiO_2 is recently found to be an excellent photocatalyst to be used in pavement engineering for reducing vehicle emission pollutants (Chen & Liu, 2010). Figure 2.1 illustrates the photocatalytic effect of TiO_2 on pavement in a transportation environment. Pollutants from vehicle exhaust adsorb to the pavement. The TiO_2 coating on the pavement surface activates with the ultraviolet sunlight to break down the pollutants. The final products are then desorbed from the pavement.

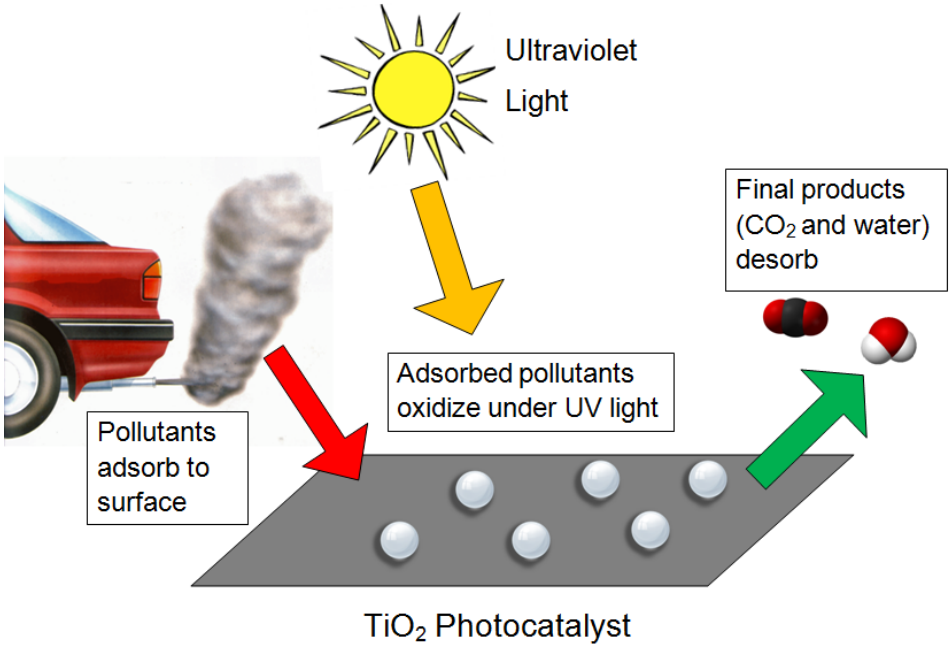

Figure 2.1: Photocatalytic effect of titanium dioxide on pavement

2.1.2 Photocatalytic Effect in Water

Not only can TiO_2 be used to remove pollutants in air, it can also be used to remove pollutants in water. Cho et al. (2006) used TiO_2 photocatalysis to treat groundwater contaminated with BTEX (benzene, toluene, ethylbenzene, xylene isomers) and TPHs (total petroleum hydrocarbons) and showed it to be an effective ex situ technique in the remediation of groundwater contaminated with petroleum. Though photocatalytic gradation of organic pollutants in water treatment works, it is difficult to separate and retrieve the small TiO_2 suspended particles (Bolt et al., 2011; Shi et al. 2009). Because this can be a major problem, Bolt et al. (2011) suggests a more suitable alternative is to incorporate TiO_2 into cementitious

construction materials, which will immobilize the TiO_2 while still allowing photocatalytic degradation to take place.

2.1.3 Hydrophilic Effect Of TiO_2

When photocatalytic oxidation decomposes staining compounds that are absorbed on a surface, the surface is cleaned and converted into a highly hydrophilic state (Hashimoto et al., 2005). Stains on the TiO_2 treated hydrophilic surface can be washed away easily, having a self-cleaning function, as the water flushes between the stain and the hydrophilic TiO_2. Surfaces that typically fog due to steam, like mirrors and glasses, can be de-fogged by the hydrophilic TiO_2 application on the surface. Titanium dioxide films on glass can oxidize stains on the windows with sunlight (photocatalysis) and can remove organic or inorganic pollutants when wetted with films of water (photoinduced superhydrophilicity) (Puzenat, 2009).

2.1.4 Asphalt & Concrete Pavement Coating

Chen and Liu (2010) found nano-TiO_2 to be capable of purifying vehicle emissions in a real traffic environment. They reported NOx removal from vehicle emissions when TiO_2 was applied to asphalt pavement. Purifying NO and NO_2 from vehicle-emitted NOx showed good decontaminating effects, with a photocatalytic rate higher than 20%. When humidity gradually increased, decontamination of NOx through TiO_2 increased. When the environment was dry (little moisture), water molecules had difficulty forming film on the TiO_2 surface. In the range of 0 to 1 mW cm^{-2} of UV intensity, the photocatalytic reaction rate increased linearly. In the range of 2 to 4 mW cm^{-2} of UV intensity, the photocatalytic reaction rate increased by square root of UV intensity. The contrast experiment (outdoor) yielded a NOx decontaminating rate between 6% and 12%.

Though TiO_2 treatment on pavements has been proven to remove pollutants from vehicle emissions (Chen & Liu, 2010), research is still being conducted on making the TiO_2 treatment resistant against vehicle traffic and natural weathering on pavements. A Louisiana study reported three different methods for applying TiO_2 to the surface of traditional concrete pavement (Hassan et al., 2010). They applied a cement-water coating with sand fines and TiO_2 nanomaterial (Cristal Millennium PC105), an ultra-thin water-based TiO_2 coating (PURETI), and sprinkled nano-sized TiO_2 particles to the fresh concrete surface prior to curing. The cement-water coating with 5% content of TiO_2 had the highest NO removal, producing 26.9% efficiency of NO removal before applied abrasion, and maintaining above 20% efficiency of NO removal after rotary abrasion and loaded-wheel tests. The NO removal was tested for 5 hours using an environmental setup with room temperature, 50% humidity, fluorescent lamps, a flow rate of 9 L/min, and an initial NO concentration of 410 ppb.

In Hong Kong, TiO_2 coated concrete paving blocks were exposed to environmental conditions for 4 months and 12 months at 5 different pedestrian roads (Chai-Mei Yu, 2003). The photocatalytic activity of the TiO_2-coated paving blocks decreased in heavy pedestrian traffic areas, as contaminants accumulated on the surface (Chai-Mei Yu, 2003). The non-pedestrian areas did not significantly affect the NO_x removal activity of the paving blocks. Washing the blocks with water did not fully recover the photocatalytic activity. Reactive surface area was lost from the accumulation of dust, dirt, oil, grease, and even discarded chewing gum (Chai-Mei Yu, 2003).

Ramirez et al. (2009) tested eight different cementitious material sample types coated with two different TiO_2 coating techniques: dip-coating and sol-gel. They tested the toluene removal efficiency and weathering resistance, characterized by different flows of water and air to

simulate real rain and wind conditions. Four of the sample types were commercial materials, which included concrete and plaster materials mainly used for wall and floor covering. The other four sample types were substrate materials, which included one commercial autoclaved white concrete material and three other concrete tiles manufactured with different finishing techniques. As samples were coated with TiO_2, the dip-coating method involved dipping the samples in a TiO_2 suspension in ethanol (0.05 g/mL). The sol-gel method involved immersing the samples into a mixture of titanium diisopropoxide bis (acetylonate) (24 mL), isopropanol (171 mL) and water (5 mL). The TiO_2 coated top-side of each sample had a surface area of 80 cm^2, and all other sides of each sample were sealed with a water dispersed epoxy coating. After testing the toluene pollutant removal in a flow-through chamber with an 18 W UV lamp and toluene inlet concentration of 12.3 ± 1.2 ppmv, the highest toluene removal efficiency was 86.2 ± 0.4 % from the autoclaved aerated white concrete dip-coated sample.

2.1.5 Factors Affecting Photocatalytic Effect

Photocatalysis can be affected by environmental factors, such as light wavelength and intensity, relative humidity, temperature, and wind. The best results for the photocatalytic effect are with higher temperatures and light intensities greater than 300 nm (Katzman, 2006). An optimal condition to remove air pollutants would be a hot summer day with low relative humidity and no wind.

Factors that can affect the photocatalytic effect of TiO_2 when applied to concrete may include porosity, humidity, aggregate type, aggregate size, application method, and applied wear. Ramirez et al. (2009) observed better retention of TiO_2 particles on the sample surface and a higher toluene removal efficiency when samples had higher porosity. Higher humidity was

reported to have lower efficiency in nitric oxide removal (Dylla et al., 2010). Coatings without fines were reported to have higher nitric oxide removal efficiency than coatings with fines (Dylla et al., 2010). As reported in the concrete application study by Hassan et al. (2010), because the weathering simulation exposed some of the TiO_2 particles embedded in the surface, applying the loaded-wheel test seemed to improve the nitric oxide removal efficiency. Applying rotary abrasion seemed to decrease the nitric oxide removal efficiency.

2.1.6 Other TiO_2 Applications

Various construction materials for NOx removal exist for both indoor and outdoor environments. As cited by Chen et al. (2007), a commercial mineral paint with 3% TiO_2 achieved a nitrogen oxide removal rate of 0.21 $\mu g/m^2 s$. A translucent paint with 5% TiO_2 achieved a nitrogen oxide removal rate of 0.06 $\mu g/m^2 s$. Floors painted with a layer of NO removing paint were reported to be effective in NO removal. For outdoor applications, photocatalytic paving was said to be more effective than planting trees, decomposing 15% of nitrous oxide from cars along the roadway. Air purification panels were said to be suitable for placing near roads to remove NOx from cars. Sound-proof walls along roadways have been reported as a surface for photcatalytic material application. In California, Toto Frontier USA uses TiO_2 to make self-cleaning ceramic tiles for use in places like hospitals and public restrooms, where it is vitally important to keep clean (Frazer, 2001). TiO_2 can also be used to treat the air and prevent fruits, vegetables, and cut flowers from spoiling and increase shelf life in storage areas (Frazer, 2001). Mitsubishi Materials Corporation in Japan developed paving stones called “Noxer” blocks that use TiO_2 to remove NOx from the air (Frazer, 2001).

Other uses for TiO_2 include detoxification of wastewater used for rice hull disinfection, water treatment of hydrophonic culture systems, treatment of VOC-polluted soils, and efficient water evaporation from hydrophilic surfaces (Hashimoto et al., 2005).

2.1.7 TiO_2 Cost

In the United States, there is little commercial availability of photocatalytic building materials (Katzman, 2006). As of 2006, Titanium Dioxide air pollution-reducing products were best found from Essroc (a North American subsidiary of Italcementi) and Green Millenium (based in California). A U.S. based company formed in 2004, PURETi, uses an electrostatic sprayer to adhere a water-based TiO_2 to a variety of surface types. PURETi products are applied to keep surfaces clean, such as buildings, aircraft, ships, curtains, carpets, and windows.

Using titanium dioxide coating can be quite expensive, however, with time and increase in demand, it is expected that the cost will decrease, as there will be more producers with this technology. As of year 2010, the average market price of ultrafine/nano titanium dioxide was $9.07/lb (Dylla et al., 2010).

2.1.8 TiO_2 Maintenance

The performance of NOx removal can be self-maintained. Calcium nitrate that accumulates on the surface can be washed away by rainfall (Chen et al., 2007). In a photocatalytic reaction with titanium dioxide, the TiO_2 does not get consumed in the reaction; so it can theoretically be used indefinitely.

Studies are still being conducted on the best application method for titanium dioxide on pavements to resist against traffic loading and natural weathering. The first air purifying concrete and asphalt pavement to be laid in the United States was laid at Louisiana State University in December 2010 (Berthelot, 2010). There were 0.25 miles of the photocatalytic asphalt pavement

laid on Aster Street and 0.25 miles of the concrete pavement on the campus. An ultra-thin water-based TiO_2 coating (PURETI) was used on both of the pavements. Before field implementation, laboratory evaluation conducted at Louisiana State University showed 25.0% efficiency of NO removal with the PURETI coating on concrete specimens (Hassan et al., 2010) and 39 to 52% efficiency of NO_x removal using the PURETI coating on warm-mix asphalt specimens (Hassan et al., 2011).

2.2 PERVIOUS CONCRETE

Pervious concrete is concrete with high porosity, which allows water to infiltrate completely through it. It is composed of coarse aggregates, cement, and water. The high void content in pervious concrete is maintained by using aggregates that are generally all one size to avoid filling the voids with fines. The single-diameter aggregates form a framework for pervious concrete (Yang & Jiang, 2002), and the aggregates are bound together with cement paste, as shown in Figure 2.2.The voids maintained throughout the structure due to the single-diameter aggregates being held together with the thin cement paste allow air or water to penetrate through the pervious concrete. Because the cement paste that binds the structure together is thin, this reduces the strength of pavement. For this reason, pervious concrete would not be appropriate for highway use, as it would need to accommodate for a high volume of heavy vehicle traffic each day. It could however be implemented on the highway shoulders, which do not carry the repetitive loads of vehicle traffic each day. Also, because pervious concrete has numerous voids exposed to the surface, it is prone to clog with debris, which could hinder water from infiltrating through the structure. This can be prevented with proper maintenance techniques.

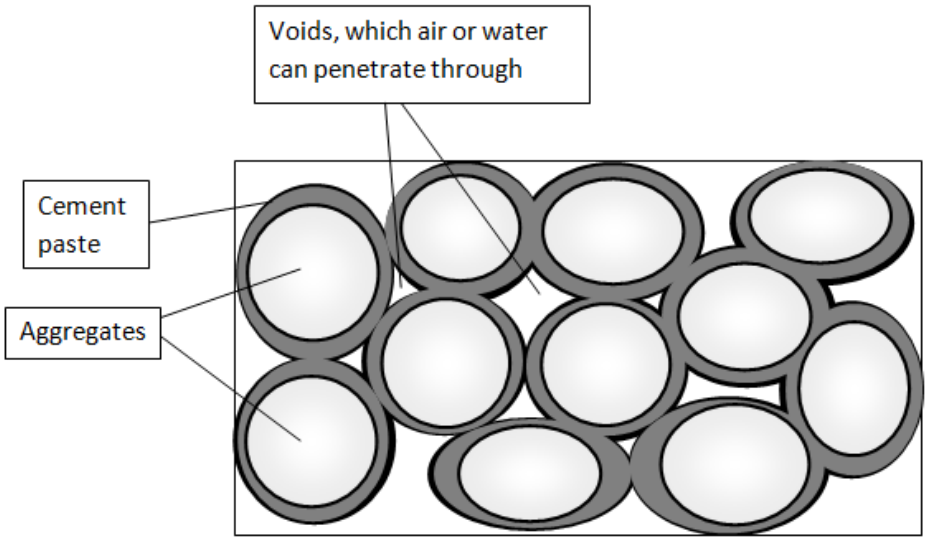

Figure 2.2: A schematic diagram of pervious concrete structure

2.2.1 Pervious Concrete Applications

Pervious concrete can be applied to footpaths, parking lots, paths in parks, shoulders, tennis courts, patios, slope stabilization, swimming pool decks, green house floors, zoo areas, drains, noise barriers, driveways, friction course for highway pavements, and low volume roads (Obla, 2007). It can also be used to allow green growth, such as placing it onto the ocean floor to form man-made seaweed and fish reefs and revive the disappearing marine environment due to pollution and exploitation (Li, 2011). The porous base is favorable to the seaweed's clinging, which in turn provides the feeding grounds that the fish and shellfish need.

2.2.2 Advantages of Pervious Concrete

Pervious concrete pavement has many advantages that help improve the quality of the environment in cities. With pervious pavement installed, rainwater can filter into the ground, which replenishes groundwater resources (Yang & Jiang, 2002). Because pervious concrete is air permeable and water permeable, the soil beneath is kept wet. Trees planted in pervious concrete

parking lots will get more air and water to the roots. A large silver maple tree died in a Salt Lake City parking lot because it could not get water to its roots from the impervious concrete that surrounded it (Rocke & Bowers, 2009). Driver comfort and safety is addressed, as permeable concrete will absorb noise from tire-to-pavement interaction and also reduce the hydroplaning effect during high rains. In the winter, snow can drain through the pervious concrete as it starts to melt, reducing the amount of snow left on the surface when compared to traditional non-pervious pavements. Pervious concrete will not have a significant contribution to the urban heat island effect like traditional non-pervious pavements do. Due to its unique void structure, pervious concrete has an insulating capability during the daytime heating cycle, as base temperatures remain similar to cooler surfaces like soil and lighter concrete (Haselbach, 2009).

Not only can pervious concrete be environmentally friendly, but it can also be aesthetically pleasing. For the 2008 Olympics in Beijing, China, about 2.7 million square feet of multi-colored pervious concrete was installed in dock frontage for the rowing and sailing venue (Rocke & Bowers, 2009). The bottom "lift" layer used larger aggregates, and the top layer used smaller aggregates that were colored.

2.2.3 Pervious Concrete Cost & Maintenance

Pervious concrete is made of the same materials as regular concrete, which includes cement, aggregate, and water, so the materials cost is about the same for both concrete types. There would be a difference in the proportions, as pervious concrete will use less cement, no fines, and more aggregate than regular concrete. Even though the first use of pervious concrete was in 1852 (Ghafoori & Dutta 1995; Obla, 2007), it is still a relatively new concept in some areas of the country. Because it may be unfamiliar to some manufacturers, this may cause it to be more costly for preparation work and installation. However, in the long term, the benefits will

pay off. Installing pervious concrete may reduce costs in installing drainage and storm water systems. Costs can range from $2 to $6.50 per square foot of installed pavement ("Permeable or Pervious Pavers Cost Comparison," n.d.).

Pervious concrete may require annual cleaning to unclog the pores. Cleaning options may include vacuuming or pressure washing to clear out debris from the voids ("Inspection and Maintenance," n.d.).

2.3 PERVIOUS CONCRETE WITH TiO_2

Most existing studies have focused on applying TiO_2 on non-pervious pavements. This places some challenges in improving the photocatalytic effect due to several reasons. Since direct interaction of TiO_2 with UV light is very critical, mixing TiO_2 into traditional concrete can only have limited NO_x reduction effectiveness at the air/solid interface. The process was observed to improve after the concrete material was abraded (some cement paste was peeled off and more TiO_2 was exposed at the surface) (Hassan et al., 2010). The durability of the photocatalytic effect becomes another challenge if TiO_2 is applied to highly trafficked highways through surface material adhesion. The dynamic tire-pavement interaction under shear and abrasion impact can dislodge coated TiO_2 particles at the surface, leaving untreated pavements. Therefore, to maximize the effect of air purification in pavements through the TiO_2 photocatalytic reaction, coating TiO_2 on the substrate of pervious concrete could have a number of benefits. As compared to traditional concrete pavements which have low porosities and relatively smooth surface textures, pervious concrete pavements have much higher porosities and rougher surface features. Figure 2.3 illustrates how TiO_2 particles can stay protected within the pores of the pervious concrete during traffic loading. The higher void ratio and the increased concave surface texture

(due to surface voids) with more surface area could enhance the bonding and durability of the applied TiO_2 at the surface, reduce impacts due to traffic abrasion and climate (snow, ice, water, heat, etc.), and increase the direct contact between TiO_2 and natural light. At the same time, pervious concrete pavement allows water to infiltrate completely through it so that rainwater can filter into the ground and replenish groundwater resources (Yang & Jiang, 2003). Installing pervious concrete may reduce costs in installing drainage and stormwater systems, reduce the urban heat island effect and noise, improve roadway skid resistance, and prevent hydroplaning. In summary, TiO_2 treated pervious concrete pavement can be widely used for pedestrian sidewalks, bike lanes, parking lots, roadway shoulders, and urban low traffic streets for its stormwater benefits and air quality purification, resulting in a greener urban living environment.

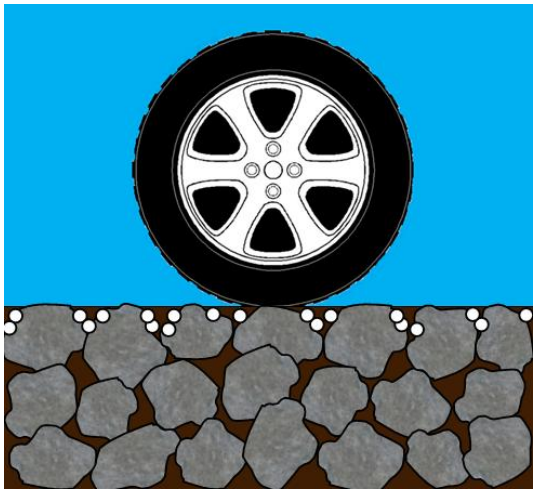

Figure 2.3: TiO_2 particles are protected in the pervious concrete pores against traffic abrasion

CHAPTER THREE

RESEARCH PROCEDURES

This research involves evaluating the environmental effectiveness of a variety of TiO_2 surface treatments on pervious concrete pavement. The goal is to find a treatment method that works the most effectively in a real traffic environment. To achieve the research goal, a four-step research procedure is followed: 1) mix design and sample preparation; 2) measurement of porosity and infiltration for untreated samples; 3) application of surface treatment; and 4) evaluation of the application methods based on infiltration tests, environmental chamber tests, and freeze-thaw tests.

3.1 PERVIOUS CONCRETE MIX DESIGN AND SAMPLE PREPARATION

3.1.1 Sample Geometry and Mix Design

Two sets of pervious concrete samples were prepared in this study. The first set of samples were trial samples to screen out potential TiO_2 application methods from a number of candidate application methods, including a cement-aggregate mix, a driveway protector mix, a cement-water slurry, TiO_2 sprinkled on top of fresh concrete, TiO_2 sprinkled on top of driveway protector, and TiO_2 mixed in water. These trial samples were each approximately 12.14 inches long, 6.51 inches wide, and 2.72 inches thick (308.4 mm x 165.4mm x 69.1mm) and were made in three batches: WMA, WMB, and WMS. All three batches were prepared in the same way but on different days. The trial samples were made using single-sized 3/8 inch – diameter aggregates, Type I Portland cement, and a water-cement ratio of 0.30. The water-cement ratio was chosen based on previous work, which gave a porosity of 22%. The pervious concrete was prepared

following the pervious concrete preparation procedure outlined in Appendix A. Specimens were lightly compacted as typical in pervious concrete placements, and designed for a target porosity of 22%. The samples were covered and left to cure for 7 days.

The second set of samples was samples made for final evaluation. These samples were made after screening out potential TiO_2 application methods that proved their effectiveness on the trial samples, which included a cement-water slurry, a driveway protector mix, TiO_2 mixed in water, and a cement-aggregate mix. Two other application methods that were not included in the trial samples, a commercial water-based TiO_2 and the PURETI commercial water-based TiO_2, were also included in the final-evaluation samples. The final-evaluation samples were approximately 12 inches long, 6 inches wide, and 2 inches thick (304.8 mm x 152.4mm x 50.8mm) and were made in three batches: WMC, WMT, and WME. All three batches were prepared in the same way but on different days. Samples were made using No. 4 sieve size (4.75 mm) narrowly graded aggregates, Type I Portland cement, and a water-cement ratio of 0.29. The pervious concrete was made following the pervious concrete making procedure outlined in Appendix A. Specimens were lightly compacted as typical in pervious concrete placements, and designed for a target porosity of 25%. The mix design for the final-evaluation samples was based on the same previous work used to determine the mix design for the trial samples. As a result, the porosity turned out to be slightly higher for the final-evaluation samples, possibly due to the use of smaller-sized aggregates. The previous work had used aggregates similar in size to the trial samples. The samples were covered and left to cure for 7 days. In addition, one traditional (non-pervious) concrete sample labeled WMD1, which was the same size as the final-evaluation samples, was prepared as a control sample with a water-cement ratio of 0.48. A summary list of all of the concrete samples that were made is shown in the Table 3.1.

Table 3.1: Summary table of concrete samples made

Sample(s)	sample type	Sample size	Aggregate size (mm)	water-cement ratio
Trial Samples				
WMA1-WMA10 WMB1-WMB10 WMS1-WMS5	pervious	308.4mm x 165.4mm x 69.1mm	9.5	0.298
Final-Evaluation Samples				
WMC1-WMC14 WMT1-WMT3 WME1-WME13	pervious	304.8mm x 152.4mm x 50.8mm	4.75	0.292
WMD1	non-pervious	304.8mm x 152.4mm x 50.8mm	4.75	0.48

.

Blocks made out of concrete were made for both sample sets, the trial samples and the final-evaluation samples, to use as forms for top compaction. These compactor forms were used to compact the pervious concrete samples by placing the form on top of each sample that was freshly poured into its mold and then tapping the top of the compactor form with a rubber mallet hammer.

Prior to making the pervious concrete samples, the amount of pervious concrete material to place into each sample mold prior to compaction and the amount of each material needed (cement, water, and aggregates) to make the pervious concrete had to be calculated.

3.1.2 Sample Preparation Method

The preparation of pervious concrete consists of 3 steps:

Step 1. Estimate sample volume

The average volume for the trial samples and the final-evaluation samples were calculated to be 3358 cm^3 and 2401 cm^3 respectively.

Step 2. Estimate mass per sample mold

Once the volume was calculated, the next step was to calculate how much material to put into each mold when making the samples. The volume that was previously calculated was the same volume that the samples were to be compacted to. With that, the amount of fresh mass to compact within each mold was calculated. Calculations were based on previous work, which the previous samples had 22% porosity. 22% porosity was chosen for this research because it was a value representative to what is practiced in the field. Typically in the field, 15-25% voids are achieved in hardened pervious concrete ("Pervious Concrete Pavement: An Overview," n.d.). Variation is expected in the sample-making process, but the samples should not have a porosity that is too low, so 18% was chosen as the minimum porosity allowed. The minimum mass allowed to get 22% porosity and the maximum mass allowed to get 18% porosity were determined. The minimum and maximum masses allowed, with the mass of the mold included, for the trial samples were calculated to be 6550 g and 6800 g respectively. The minimum and maximum masses allowed, with the mass of the mold included, for the final-evaluation samples were calculated to be 4721 g and 4950 g respectively.

Step 3. Estimate materials per batch of samples

After the total amount of mass to place in each sample mold had been calculated, it is necessary to determine the weight of each material (cement, water, and aggregates) to make a batch of pervious concrete samples. These materials-per-batch calculations were based on the same previous work used to perform the mass-per-mold calculations, which the samples had 22% porosity. To account for any material lost while mixing and handling the pervious concrete, 20% extra and an alternative estimate with 30% extra were added into the calculations.

A summary of the material proportions used to make a 10-sample batch of the trial samples and a 12-sample batch of the final-evaluation samples are shown in tables 3.2 and 3.3 respectively.

Table 3.2: Materials Proportions in Pervious Concrete (trial samples)

materials	Mass ratio to cement	Mass for 10 molds + 30% extra (lb)
cement	1	35
aggregate	4	140
water	0.30	10.43

Table 3.3: Materials Proportions in Pervious Concrete (final-evaluation samples)

materials	Mass ratio to cement	Mass for 12 molds + 30% extra (lb)
cement	1	30
aggregate	4	120
water	0.29	8.76

3.1.3 Sample Size Variation

After all the samples were cured and dry, the dimensions of each of the first-made batch of trial samples (WMA samples) were measured and compared to quantify any variation between the samples. The average depth was 69.14±1.93 mm. The average top length was 308.45±1.31 mm. The average bottom length was 299.22±1.94 mm. The average top width was 165.43±2.75 mm. The average bottom width was 154.41±2.36 mm. Due to the pre-made shape of the mold, samples were slightly longer (l) and wider (w) on the top surface than the bottom surface. The

depth (d) of each sample stayed fairly constant however. The variations in the width and length were minor and not dramatically affect any testing results.

3.2 POROSITY AND PERMEABILITY OF PERVIOUS CONCRETE SAMPLES

3.2.1 Porosity Test

The porosity test was performed on the prepared samples using the method proposed by Montes et al. (2005). Two different weights were determined for each sample: dry weight in the air (W_d) and submerged weight in the water with at least half an hour submerging time (W_s). Figure 3.1 shows the laboratory setup for determining the submerged weight of samples. The porosities (P) of the samples were calculated from the measured dry mass (W_d) and submerged mass (W_s) for each sample based on Equation 3.1, where ρ_w and V_t are the density of water and total volume of sample respectively (Montes et al., 2005).

$$P(\%) = \left(1 - \frac{\frac{W_d - W_s}{\rho_w}}{V_t} \right) \times 100 \qquad [3.1]$$

All samples within each batch were fairly consistent with porosity. Typically, an acceptable porosity for pervious concrete is between 15% and 25% voids ("Pervious Concrete Pavement: An Overview," n.d.). Of the trial samples, the porosities of the WMA samples ranged from 23.82% to 26.00%, with an average of 24.80%. The porosities of the WMB samples ranged from 20.16% to 24.25%, with an average of 22.22%. Of the final-evaluation samples, the porosities of the WMC samples ranged from 24.23% to 26.10%, with an average of 25.13%. The porosities of the WME samples ranged from 24.65% to 26.45%, with an average of 25.34%.

Figure 3.1: Pervious concrete samples submerged underwater during porosity test

3.2.2 Infiltration Test

Pervious concrete allows water to infiltrate completely through it, as shown in Figure 3.2. The infiltration characteristics of the pervious concrete were determined before and after the surface coating applications. The test followed the ASTM Standard C1701 (2009), but was applied to the smaller scale samples by using a smaller 4-inch diameter pipe. The pipe was attached to the sample surface using plumber's putty at two locations, centered at 3 inches (76.2 mm) from the left and right sides of the sample (Figure 3.3a). 2000 mL of water was poured through the pipe (Figure 3.3b) and timed. Each side (left and right) of each sample was tested 3 times, and the overall average infiltration rate for each sample was calculated. The infiltration rate was calculated as shown in Equation 3.2, where d is the diameter of the pipe and t is the infiltration time. Infiltration rates for each sample type before and after applied surface coatings are shown in Table 4.1.

$$infiltrati\,on\,rate = \frac{\left(\frac{volume\,of\,water\,infi\,ltrated}{area\,of\,surface\,infi\,ltrated\,th\,rough}\right)}{time\,to\,fu\,lly\,infilt\,rate} = \frac{\left(\frac{2000\,\text{mL}}{\frac{\pi}{4}d^2}\right)}{t} \quad [3.2]$$

Figure 3.2: Water infiltrating completely through a pervious concrete sample

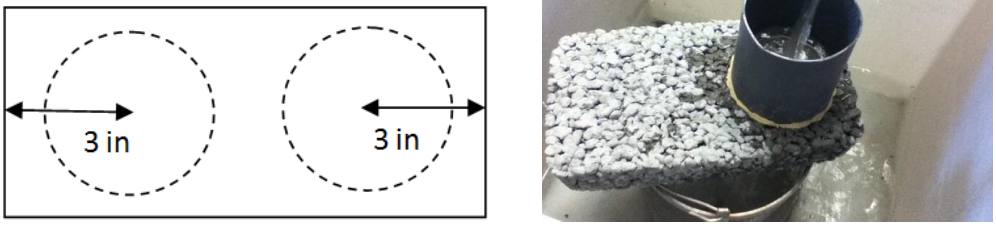

(a) **(b)**

Figure 3.3: Pervious concrete infiltration test: a) pipe positions on the sample and b) pouring water through the pipe attached to the sample with plumber's putty

The infiltration rates of the trial WMA samples were acceptable, with fast rates ranging from 17.37-26.86 mm/s. The infiltration rates of the trial WMB samples were not so fast, with

rates ranging from 3-8.55 mm/s. Though both WMA and WMB batches followed the same mix design, variation may be due to the handling of the materials, the speed at which the water was added to the mix, or the ambient temperature during the making of the pervious concrete. Figure 3.4 shows the average infiltration rate versus porosity for WMA and WMB samples. The trend shows an overall increase in infiltration rate with respect to an increase in porosity (a power law relationship), but not all points follow this trend. For example, both samples WMA4 and WMB7 had porosities of about 22%, but WMA4 had an average infiltration rate of 20.47 mm/s, and WMB7 had an average infiltration rate of 6.05 mm/s. This is different by more than 3 times as much. It is possible that the two samples with the same porosity had different infiltration rates because of differences in connectivity of the voids within the internal structure of the samples. The high degree of variability in infiltration exists because the void connectivity variability is not accounted for by porosity.

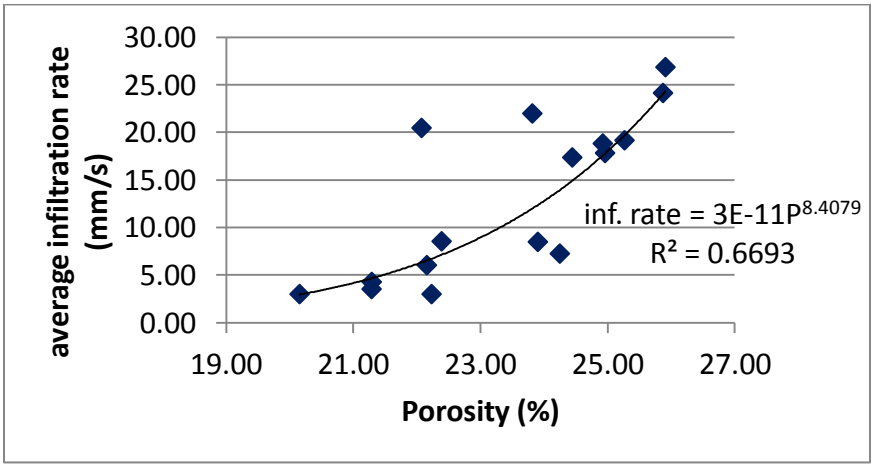

Figure 3.4: Infiltration rate vs. porosity for WMA and WMB samples

3.3 SURFACE TREATMENT USING TiO_2

3.3.1 Trial Samples

The first batches of trial samples (WMA's, WMB's and WMS's) were tested with several different TiO_2 application methods. Table 3.4 summarizes the materials applied on each of these trial samples. Ultra-fine titanium dioxide PC105 supplied by Cristal Global was used in this study for all of the surface treatments, unless otherwise noted. Six different TiO_2 coating methods were tested, with different concentrations within each of these methods:

1. C**ement/aggregate mix (CAM):** it was a thin layer of pervious concrete with finer aggregate size and TiO_2 mixed in. This could be used as a special application when surface maintenance is needed for pervious concrete.
2. **Driveway protector mix (DPM):** it consisted of a transparent liquid driveway protector (siliconate, water-based concrete sealer) and TiO_2 uniformly mixed together and brushed onto the surface of pervious concrete.
3. **Cement-water slurry high (CWSH)**: it consisted of a relatively high concentration of cement and TiO_2 mixed into water and brushed onto the surface of pervious concrete.
4. **TiO_2 sprinkled on driveway protector (SDP)**: it consisted of TiO_2 sprinkled onto driveway protector (siliconate, water-based concrete sealer) freshly painted on the surface of pervious concrete.
5. **TiO_2 sprinkled on fresh concrete (SFC)**: it consisted of TiO_2 sprinkled onto fresh pervious concrete.
6. **TiO_2 mixed in water on fresh concrete (TIWF)**: it consisted of TiO_2 mixed in water and painted onto fresh pervious concrete.

Plain pervious concrete samples with no TiO_2 (PPC) were also tested, as they were used as control specimens.

Table 3.4: Summary of surface treatments on the trial samples

Sample Name	Surface Treatment Type	ultra-fine TiO_2 (g)	Surface Material Contents (% of surface coating by weight)				
			ultra-fine TiO_2 (%)	cement (%)	water (%)	aggregate (%)	driveway protector (%)
WMA1	CAM	11.79	0.94%	17.85%	9.82%	71.39%	0
WMA2	PPC	0	0	0	0	0	0
WMA3	DPM	4.43	14.29%	0	0	0	85.71%
WMA4	DPM	14.58	16.57%	0	0	0	83.43%
WMA5	CWSH	3.36	5.01%	49.99%	45.00%	0	0
WMA6	CWSH	2.84	2.69%	51.21%	46.09%	0	0
WMA7	CAM	62.32	5.00%	17.12%	9.41%	68.47%	0
WMA8	PPC	0	0	0	0	0	0
WMA9	CWSH	5.02	5.00%	52.78%	42.22%	0	0
WMA10	CAM	139.39	9.38%	15.22%	14.53%	60.87%	0
WMB1	DPM	1.28	2.23%	0	0	0	97.77%
WMB2	SDP	0.7	1.06%	0	0	0	98.94%
WMS1	SFC	2.7	100.00%	0	0	0	0
WMS2	TIWF	3.18	4.76%	0	95.24%	0	0
WMS3	TIWF	3.35	9.08%	0	90.92%	0	0
WMS4	SFC	1	100.00%	0	0	0	0
WMS5	TIWF	7.95	19.34%	0	80.66%	0	0

3.3.2 Final-Evaluation Samples

Once testing was completed on the trial samples, the most promising application methods were selected for further testing. Other application methods were discarded due to either limited effectiveness in TiO_2 reduction (such as coatings with too much cement and not enough TiO_2 to counteract the hindrance of it), or non-durable surface coating and potential hazardous application method (such as the "sprinkled" method).

As with the first trial samples, ultra-fine titanium dioxide PC105 supplied by Cristal Global was used in surface treatments for the final evalaution samples. In total, eight application methods were evaluated for the remainder of this study, they include:

1. C**ommercial water-based TiO_2 (CWB)**: it consisted of Cristal Global's S5-300B commercial water-based TiO_2 brushed onto the surface of pervious concrete.
2. **Driveway protector mix (DPM):** it consisted of a transparent liquid driveway protector (siliconate, water-based concrete sealer) and TiO_2 uniformly mixed together and brushed onto the surface of pervious concrete.
3. **Cement-water slurry low (CWSL)**: it consisted of a thin slurry with low cement concentration and TiO_2 uniformly mixed together and brushed onto the surface of pervious concrete.
4. **Cement-water slurry high (CWSH)**: it consisted of a relatively high concentration of cement and TiO_2 mixed into water and brushed onto the surface of pervious concrete.
5. **TiO_2 in water (TIW):** it consisted of water and TiO_2 uniformly mixed together and brushed onto the surface of pervious concrete.
6. **PURETI (PUR):** it consisted of the PURETI commercial water-based TiO_2 applied to the surface with a special electrostatic sprayer by the PURETI producer.
7. C**ement/aggregate mix (CAM):** it was a thin layer of pervious concrete with finer aggregate size and TiO_2 mixed in. This could be used as a special application when surface maintenance is needed for pervious concrete.
8. C**ement/aggregate mix with higher TiO_2 concentration (CAMH)**: it was the same application method as method CAM but with higher TiO_2 concentration.

In addition, three types of control specimens were included in the testing plan for the final-evaluation samples. They included: plain pervious concrete with no TiO_2 (PPC), plain traditional concrete with no TiO_2 (PTC), and traditional concrete coated with the CWSH method (TCC). The selection of the CWSH coating method for traditional concrete was to compare the results with literature. Except for the CWB, PUR, and CAMH application methods, all methods maintained the same TiO_2 rate of $0.06 g/in^2$ ($8.61*10^{-5}$ g/mm^2). Table 3.5 summarizes the materials applied on each of these final-evaluation samples. Figure 3.5 is a photograph of some of the final-evaluation TiO_2 coated samples.

Table 3.5: Summary of surface treatments on final-evaluation samples

Surface Treatment Type	ultra-fine TiO_2 (g)	Surface Material Contents (% of surface coating by weight)					
		ultra-fine TiO_2 (%)	cement (%)	water (%)	aggregate (%)	driveway protector (%)	commercial water-based TiO_2 (%)
PPC	0	0	0	0	0	0	0
PUR		*(treatment applied commercially)*					
CWB	0	0	0	0	0	0	100.00%
PPC	0	0	0	0	0	0	0
DPM	4	14.29%	0	0	0	85.71%	0
TIW*	4.00	11.76%	0	88.24%	0	0	0
CWSL*	4.00	9.82%	9.82%	80.37%	0	0	0
CAM	4.00	0.46%	17.67%	9.23%	72.65%	0	0
CWSH	4.00	5.01%	49.99%	45.00%	0	0	0
CAMH	10	1.15%	17.18%	9.59%	72.09%	0	0
PTC	0	0	0	0	0	0	0
TCC**	4.00	5.01%	49.99%	45.00%	0	0	0

** The TIW coating was later washed off and replaced with CWSL coating*

*** The traditional concrete control was later coated with CWSH method, making it become TCC*

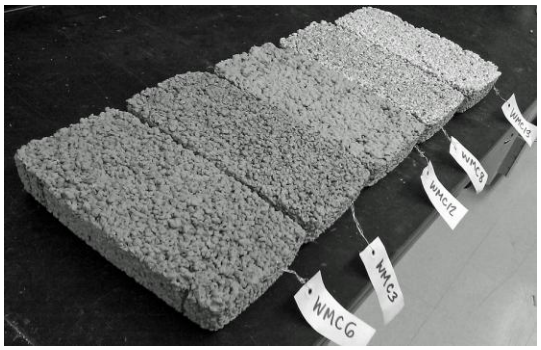

Figure 3.5: TiO_2 coated pervious concrete samples

Two specimens of each of the methods, CWB, CWSH, CWSL, DPM, PUR, CAM, CAMH, and PPC, were prepared to use in later durability tests.

3.3.3 Optimization of DPM Coating Method

Because the DPM surface coating method was found to be promising with respect to TiO_2 reduction, maintaining permeability, and withstanding de-icing agent, this method was further studied to evaluate the effect of TiO_2 concentration of NO reduction. Four different TiO2 concentration rate, 5%, 10%, 15%, and 18% were studied, and their material proportions are shown in Table 3.6.

Table 3.6: Summary of surface treatments for DPM coating optimization

Surface Treatment Type	ultra-fine TiO_2 (g)	Surface Material Contents (% of surface coating by weight)					
		ultra-fine TiO_2 (%)	cement (%)	water (%)	aggregate (%)	driveway protector (%)	commercial water-based TiO_2 (%)
DPM (5%)	1.45	5.00%	0	0	0	95.00%	0
DPM (10%)	2.9	10.00%	0	0	0	90.00%	0
DPM (15%)	4.35	15.00%	0	0	0	85.00%	0
DPM (18%)	5.22	18.00%	0	0	0	82.00%	0
PPC	0	0	0	0	0	0	0

3.4 EVALUATION OF SURFACE TREATMENT METHODS

Once the surface treatments were applied, the performance of each treatment method was evaluated against several different tests. The infiltration test was performed to evaluate the permeability of each treatment method. The environmental chamber test was performed to evaluate each treatment's effectiveness at removing pollutants from the air. Each treatment type was viewed under the Scanning Electron Microscope to determine the TiO_2 distribution on the surface. To evaluate the durability of each treatment method, samples were tested against freeze-thaw in the lab and placed outside to endure natural weathering. Two of the most resistant coatings were selected to coat segments of an actual pervious concrete pavement in the field, where their resistance was evaluated against scaling. Details of the each evaluation are discussed in Chapter 4.

CHAPTER FOUR

EVALUATION OF SURFACE TREATMENT METHODS

4.1. INFILTRATION

Infiltration rates for each sample before and after applied surface coatings are measured to determine if the surface treatment methods could reduce the permeability of the samples. For the trial samples, only one sample per treatment type was tested to obtain fast results as a screening test. For the final-evaluation samples, two repetition samples per treatment type were tested, except for DPM (5%), DPM (10%), DPM (15%), DPM (18%), and PPC (sample WME6), which were only tested once each due to time constraints. A summary of the average infiltration rates before and after applied surface coatings is shown in Table 4.1. Most coating methods maintained an acceptable level of infiltration rate for pervious concrete pavements. In practice, flow rates for water through pervious concrete are typically 480 in/hr (3.4 mm/s) ("Pervious Concrete Pavement: An Overview," n.d.). The samples in this study had mostly higher infiltration rates than this, which may be due to their high-porosity design. The TIW method was not tested for infiltration because the coating was coming off by the touch of a hand and could wash off with water.

Table 4.1: Infiltration Rates Before and After Surface Coating Applications

Surface Treatment Type	Sample(s)	BEFORE SURFACE APPLICATION Avg. Infilt. Rate (mm/s)	AFTER SURFACE APPLICATION Avg. Infilt. Rate (mm/s)	% Decrease in infiltration rate
Trial Samples**				
CWSH	WMA5	19.17	8.86	53.80%
CWSH	WMA9	18.83	1.16	93.82%
CAM	WMA7	17.83	18.25	-2.34%*
CAM	WMA10	21.99	1.63	92.59%
Final-Evaluation Samples				
CWB	WMC3, WMC4	15.40±0.49	12.23±1.00	20.60%
CWSH	WMC11, WMC12	18.27±3.28	7.62±0.01	58.29%
CWSL	WMC9, WMC13	17.40±3.09	8.44±3.08	51.50%
DPM	WMC7, WMC8	16.76±3.95	11.65±4.03	30.49%
PUR	WMC2, WMC5	15.70±2.59	13.83±2.92	11.92%
CAM	WMC10, WMC14	14.75±0.99	14.19±1.25	3.85%
CAMH	WMT1, WMT3	9.07±1.44	9.39±0.63	-3.49%*
PPC	WMC1, WMC6	15.77±1.46	-	-
DPM Optimization Samples				
DPM (5%)	WME11	20.97	17.23	17.81%
DPM (10%)	WME7	21.05	14.73	30.05%
DPM (15%)	WME9	19.02	15.03	21.02%
DPM (18%)	WME3	19.89	15.15	23.85%
PPC	WME6	20.25	-	-

- This data is not applicable. Implying no infiltration change. The negative value could be due to testing variations.*
*** Infiltration data not available for some of the trial samples*

Because the trial samples were the first to be made, their surface applications were not made efficiently, as shown with their high decrease in infiltration rates. After learning from the experience with making the first trial samples, the material proportions in the surface treatments of the final-evaluation samples were made more efficiently. The final-evaluation samples still

showed reduction in infiltration rates however. All of the final-evaluation samples except for the two cement/aggregate mixes (CAM and CAMH) had noticeable, but not significant decreases in infiltration rates. CAM and CAMH both did not change much in infiltration rate. The cement-water slurries, CWSH and CWSL changed the most, and CWB, PUR, and all of the DPM treatments each had less than 31% decrease in infiltration rate.

4.2 ENVIRONMENTAL CHAMBER

A laboratory environmental system was used to evaluate the pollutant removal efficiency due to the photocatalytic effect of the TiO_2. The setup included a 150 L Teflon chamber maintaining 75°F (23.89°C) temperature and 25% humidity, two small fans inside for uniform mixing, and six 25W black lights. Inside the chamber, the sample surface sat about 16 inches (406.4 mm) below the chamber lights. Prior to the final set-up used, different set-ups were tried, including 15W lights instead of 25W lights, a different air flow generator, and no fans.

The irradiance of the 25W lights were measured and compared to the solar irradiance on the roof in October and November (Figure 4.1). The 25W lights were within the wavelength region (below 387 nm) where TiO_2 is photoactive. Most of the 25W lights output energy was between 300-400 nm. The irradiance of the 25W lights was about 6.11 W/m^2, comparable to a cloudy fall day in Pullman, Washington.

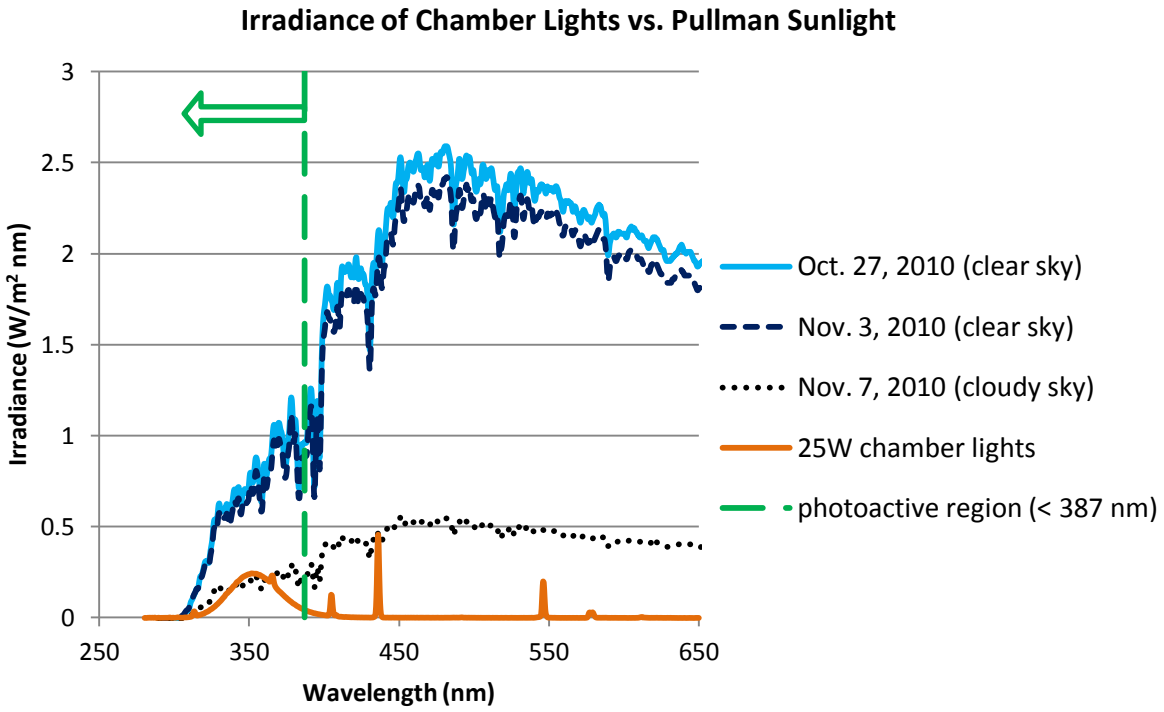

Figure 4.1: Comparison of the six photo-chamber 25W black lights and Pullman fall solar irradiances

Three different gaseous pollutants that are present in automobile exhaust were tested: toluene, trimethylbenzene (TMB) and nitric oxide (NO). Figure 4.2-a shows the chamber setup for the toluene and TMB pollutants. The chamber was a static set-up with average initial mixing ratios of approximately 43 and 35 parts per billion by volume (ppbV) mixing for toluene and TMB respectively. Toluene and TMB were injected from a syringe pump at a controlled flow rate and the dispensed liquid evaporated under a flow of warm clean air (17 SLPM) produced by an AADCO zero air generator. The mixture flowed through the environmental chamber. When the desired concentrations were reached, the flow into the chamber was closed off, the UV lights were turned on, and the reductions in VOCs were measured by a Proton Transfer Reaction Mass

Spectrometer (PTR-MS). The PTR-MS periodically sampled from the chamber over time, drawing ~ 100 mL of air from the chamber with each sampling.

The NO pollutant measurement used a flow-through experiment (Figure 4.2-b). The average initial concentration of NO was approximately 410 ppbV and the air flow rate was 17 L/min. NO from a compressed gas cylinder (Scott Marrin Inc) containing 500 ppmV of NO was diluted to 410 ppbV using mass flow controllers. The air flowed continuously through the chamber and NO was measured at the chamber exit. When the steady-state concentration of NO was reached, the UV lights were turned on and the reduction in the pollutant concentration was measured by the TECO NO_x analyzer.

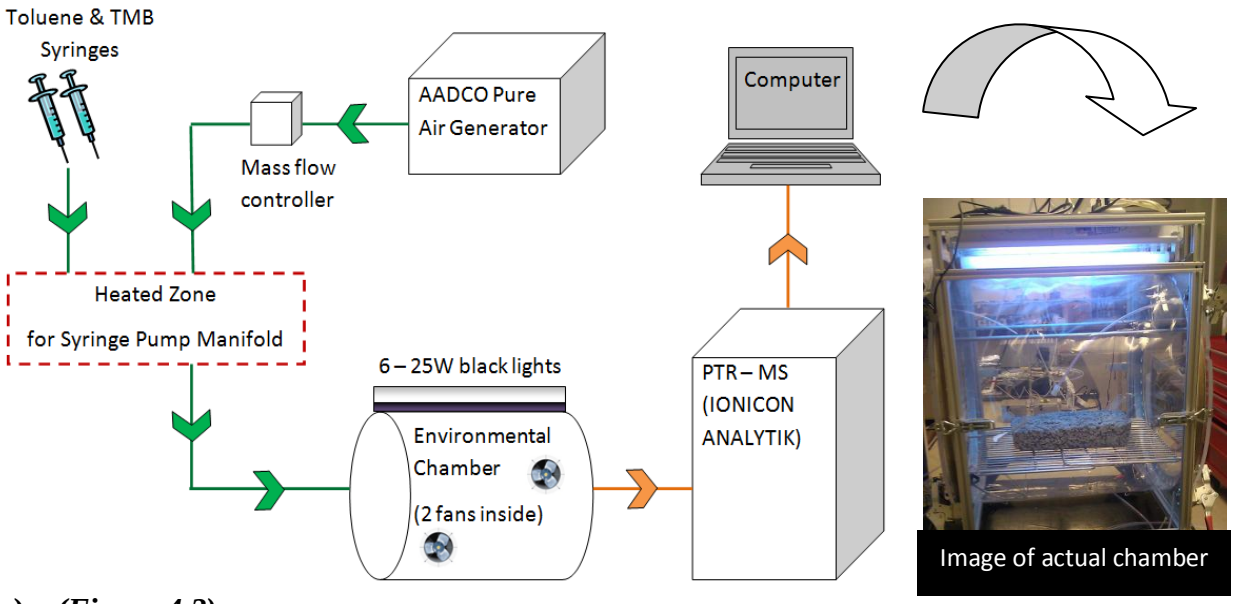

(a) ***(Figure 4.2)***

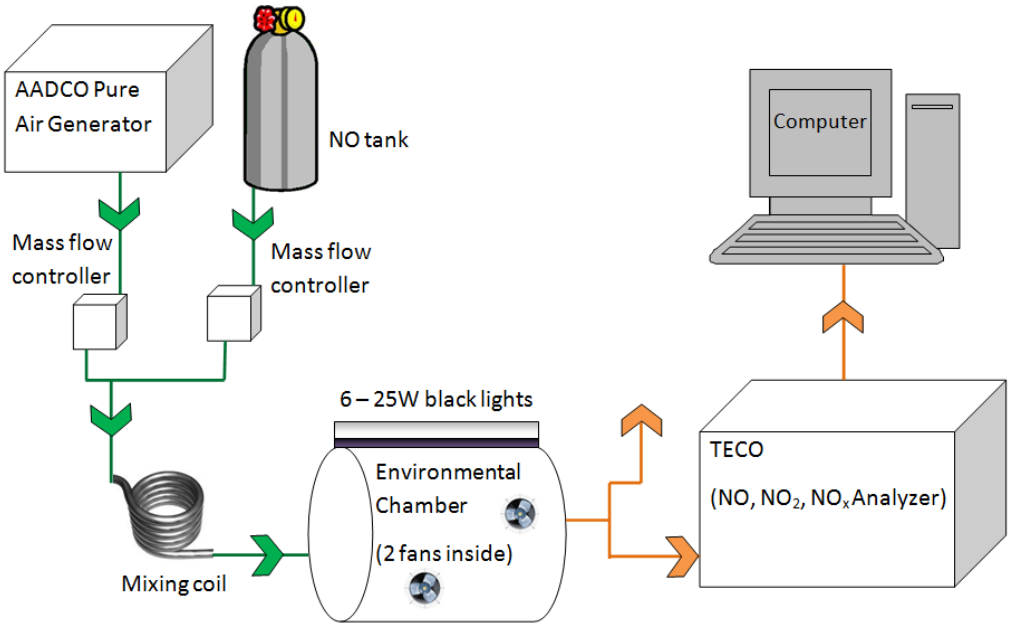

(b)

Figure 4.2: Environmental chamber set-up for (a) Toluene and TMB injection and (b) NO injection

4.2.1 Chamber Results

4.2.1.1 Trial samples chamber results

The first trial samples were tested with toluene and TMB. Initially, samples were tested with 15W lights, and only toluene was injected into the chamber. Because the lights had a relatively low output comparing to the natural solar irradiance, the lights were upgraded to 25W lights and TMB was also introduced into the chamber with toluene. The chamber results for each of the three pollutant types, toluene, TMB, and NO, are presented in terms of percent reduction of the pollutant, calculated as shown in Equation 4.1, where X is the measured molar mixing ratio in units of parts per billion by volume (ppbV).

$$\% \text{ Reduction} = \left(\frac{X_{final} - X_{initial}}{X_{initial}} \right) * 100\% \qquad [4.1]$$

Figure 4.3 shows the some of the trial samples tested with 15W lights with toluene. Figures 4.4a and 4.4b show the other trial samples tested with 25W lights with toluene and TMB respectively.

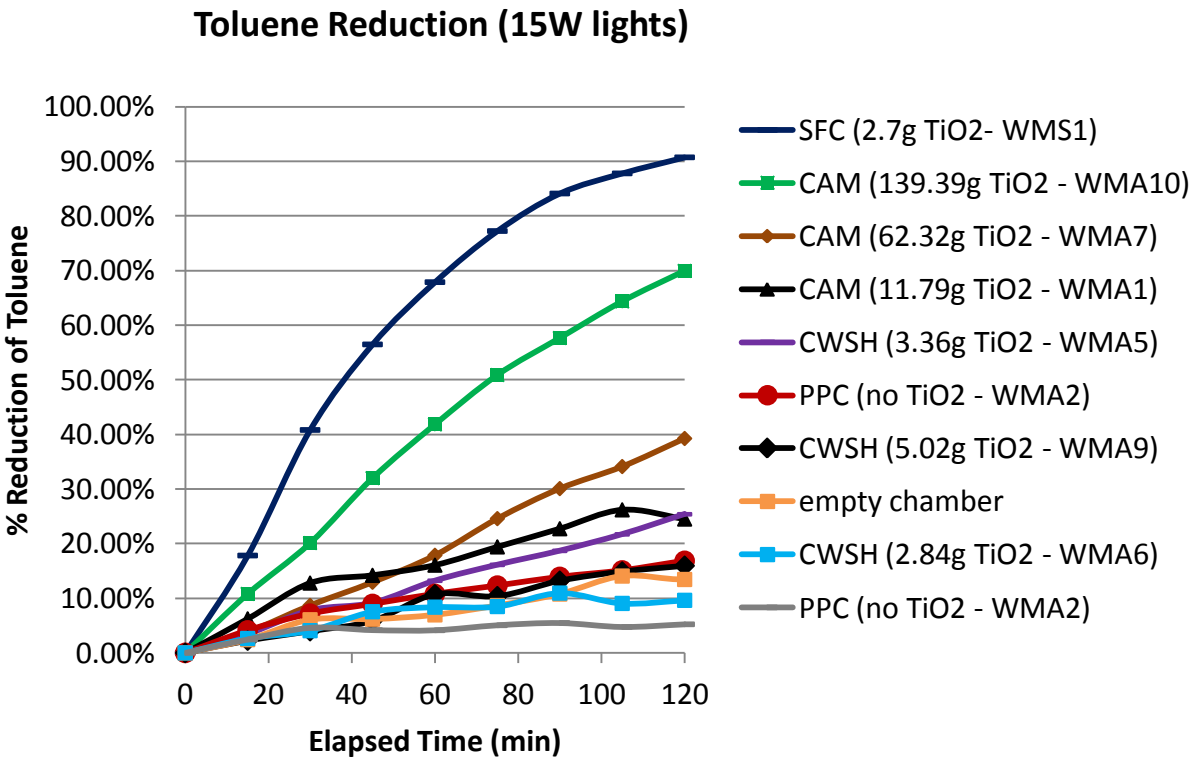

Figure 4.3: Static chamber results for trial samples tested with 15W lights with toluene

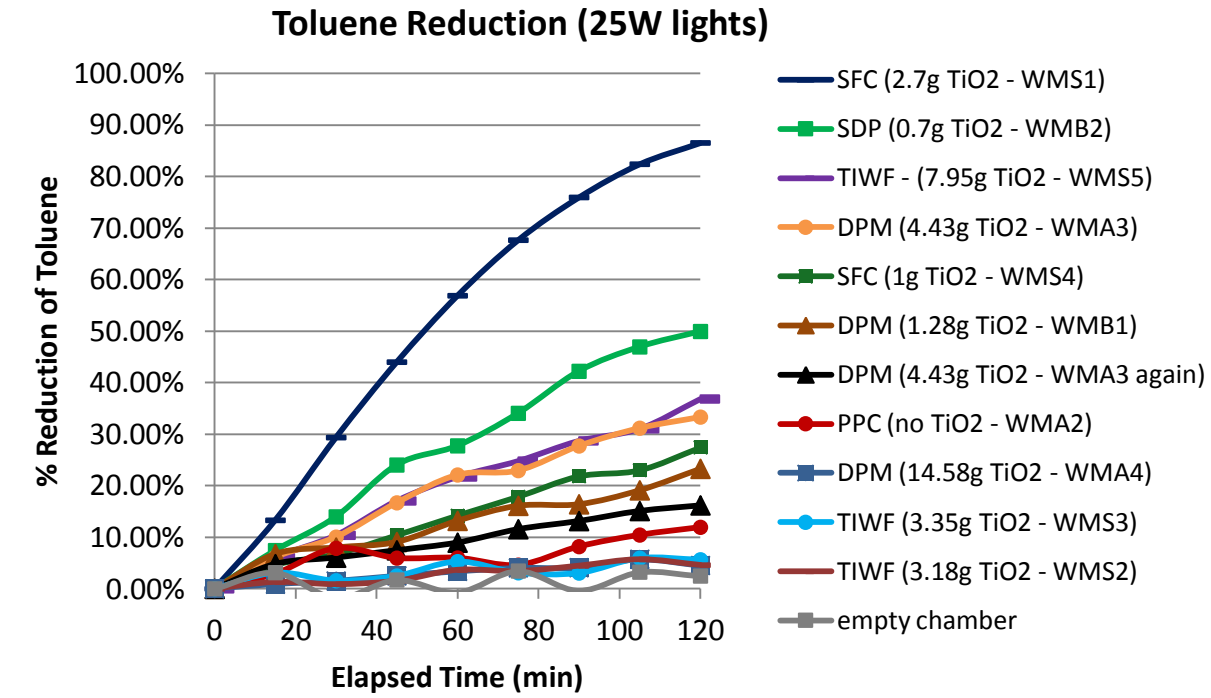

(a)

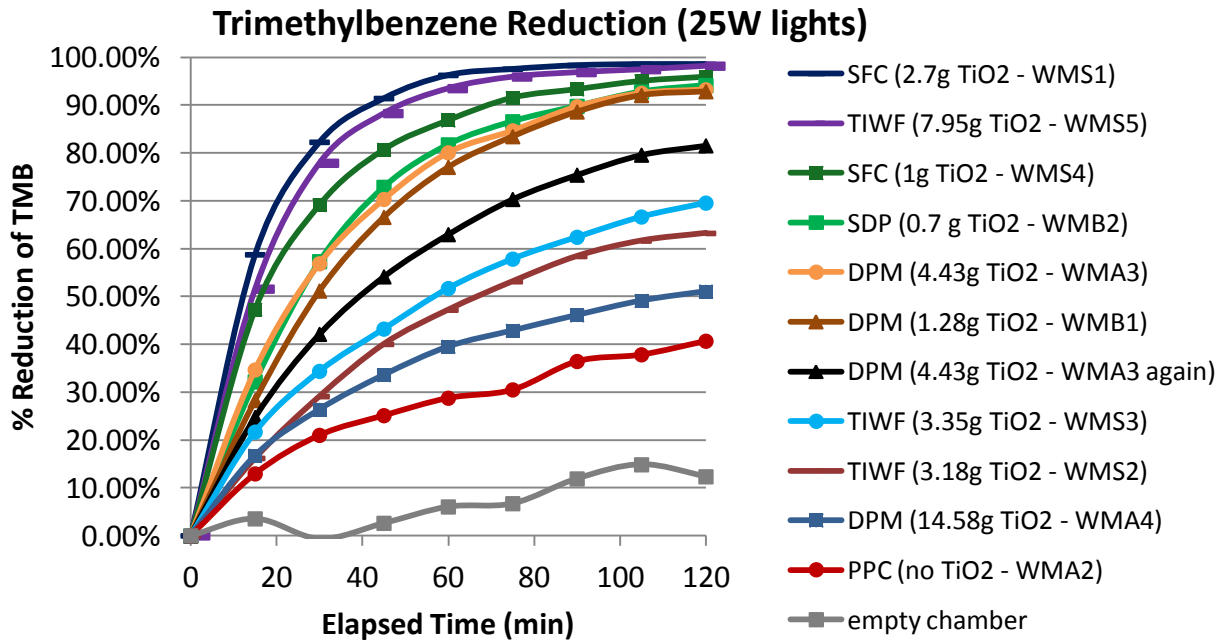

(b)

Figure 4.4: Static chamber results for trial samples tested with 25W lights with a) Toluene and b) TMB

There were two samples in common that were tested under both 15W lights and 25W lights. The trial sample SFC with 2.7 g of TiO_2 on it and the PPC trial sample did not show dramatic differences between the 25W lights and the 15W lights used. Figure 4.5 shows how the two samples ranked when placed in the chamber with Toluene and TMB under 15W lights and under 25W lights. With the PPC sample, the 25W lights ranked higher in reduction of both Toluene and TMB. With the SFC sample, the 15W lights ranked higher in reduction of Toluene. It is possible that the 15W lights ranked higher in Toluene reduction because the 25W lights may be defective and are not outputting the amount of light that they should. It is also possible that the SFC sample was highly reactive no matter what light source it was under and for that reason, its toluene reduction was similar under both lights.

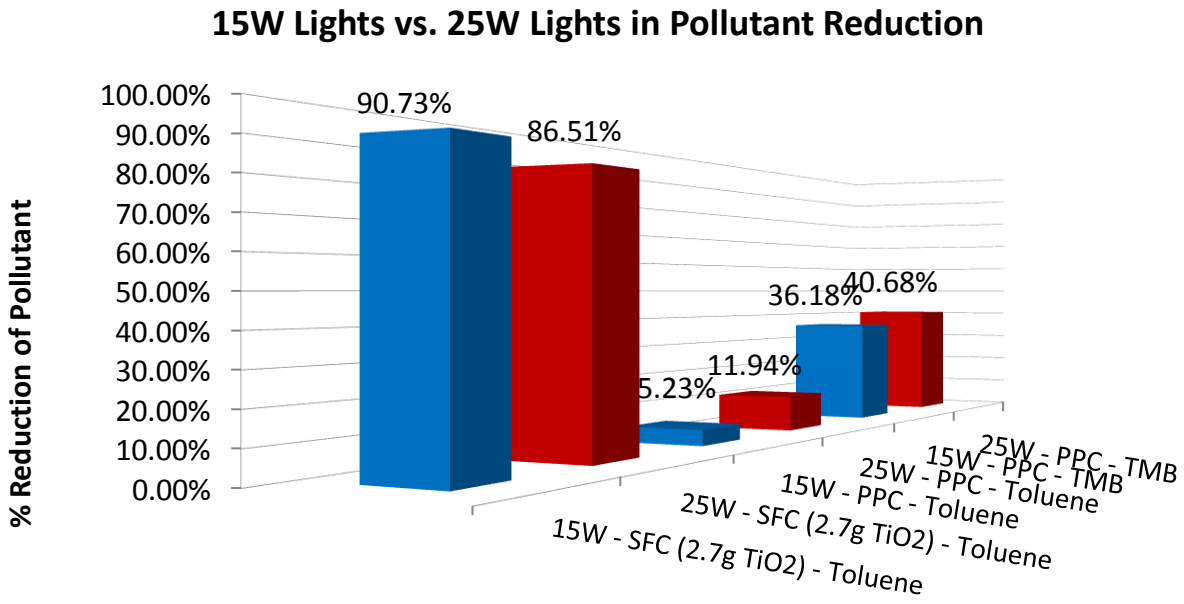

Figure 4.5 Differences in pollutant reduction with 15W lights vs. 25W lights

Under 15W lights, the highest toluene reductions were seen with TiO_2 sprinkled on fresh concrete (SFC), and a cement/aggregate mix (CAM) (samples WMS1 and WMA10 respectively) both providing over 69% static Toluene reduction. Under 25W lights, the highest Toluene reductions were seen with TiO_2 sprinkled on fresh concrete (SFC) and TiO_2 sprinkled on driveway protector (SDP) (WMS1 and WMB2 respectively) both with over 49% static Toluene reduction. The highest TMB reductions (under 25W lights) were seen with TiO_2 sprinkled on fresh concrete (SFC), TiO_2 mixed in water on fresh concrete (TIWF), TiO_2 sprinkled on driveway protector (SDP), and TiO_2 mixed in driveway protector (DPM), each with over 92% static TMB reduction . As shown in the results, when TiO_2 was sprinkled on the surface, it had more direct exposure to the air, hence it was most effective at removing pollutants. At the same time, TiO_2 sprinkled directly on the surface of fresh concrete and on driveway protector did not stick well and the TiO_2 particles would instantly come off with the touch of a hand.

Even though certain applications methods appeared better at reducing pollution than others, results also show that the higher the TiO_2 concentration, the better the pollutant reduction. For this reason, it is important to perform additional testing with a constant amount of TiO_2. After the first larger-sized sample testing, 3 to 5 g of TiO_2 showed a sufficient amount of reduction with different application methods, so 4g of TiO_2 was selected as the constant amount of TiO_2 for mixes in the next smaller-sized sample testing.

4.2.1.2 Final-evaluation samples chamber results

The final-evaluation samples were tested with toluene, TMB, and NO. All of the final-evaluation samples were tested with 25W lights. A summary table of the average chamber results for each treatment type before any applied abrasive effects is shown in Table 4.2. Note that the results shown for the pervious concrete samples are an average of at least two samples tested per

surface treatment type. Figure 4.6 shows the graphical results of toluene and TMB. Figure 4.7 shows the graphical results of NO. Because the NO was applied as a flow-through experiment, a relationship was found to convert the flow-through data into static data. A flow-through chamber at steady-state concentration has the relationship in Equation 4.2, where $C(t = \infty)$ is the concentration at steady state, C_{in} is the initial ambient concentration, n is the exchange rate (air flow rate per volume, 17 SLPM/150 L), and k is the decay rate due to chemical oxidation (hr^{-1}).

$$C(t=\infty) = \left[\frac{C_{in}n}{n+k}\right] \qquad [4.2]$$

The equation for describing the rate of change in the static experiments is stated in Equation 4.3, where C(t) is the chamber concentration at time t, C_0 is the initial chamber concentration, and k is the same decay rate, as found in the flow-through relationship.

$$C(t) = C_0 e^{-kt} \qquad [4.3]$$

Table 4.2: Summary Chamber Results for Final-Evaluation Samples Before Abrasion

Sample	TiO_2 (g/m^2)	% of surface coating that is TiO_2	Static Chamber (120 min)		Flow-through Chamber (29.83 min)	NO decay rate, k (1/hr)	Converted Static Chamber (29.83 min)
			total % toluene reduction	total % TMB reduction	Total % NO reduction		Total % NO reduction
empty chamber	-	-	2.48%	12.35%	1.38%	0.09	4.61%
PPC	-	-	15.06±0.28%	29.86±8.83%	2.51±0.19%	0.17	8.31%
PTC	-	-	-	-	1.61%	0.111	5.37%
TCC	86.1	5.01%	-	-	13.95%	1.102	42.19%
CWB	527 *(water-based TiO_2)*	100% *(water-based TiO_2)*	61.86±14.06%	94.64±1.85%	52.46±2.07%	7.50	97.59%
CWSH	86.1	5.01%	13.23±1.62%	81.65±1.50%	35.97±1.64%	3.82	85.04%
CWSL	86.1	9.82%	78.82±9.22%	97.26±0.63%	50.79±0.49%	7.01	96.94%
DPM	86.1	14.29%	61.65±10.77%	93.87±1.09%	53.27±3.63%	7.79	97.92%
TIW	86.1	11.76%	91.98±3.08%	96.34±1.08%	51.30±2.43%	7.15	97.14%
PUR	2.02	-	43.42±1.79%	89.50±4.05%	48.29±3.13%	6.37	95.79%
CAM	86.1	0.46%	21.62±4.30%	68.28±5.99%	19.11±3.46%	1.62	55.35%
CAMH	217	1.15%	-	-	32.97±1.73%	3.34	81.03%

- This data is not applicable or is unavailable.

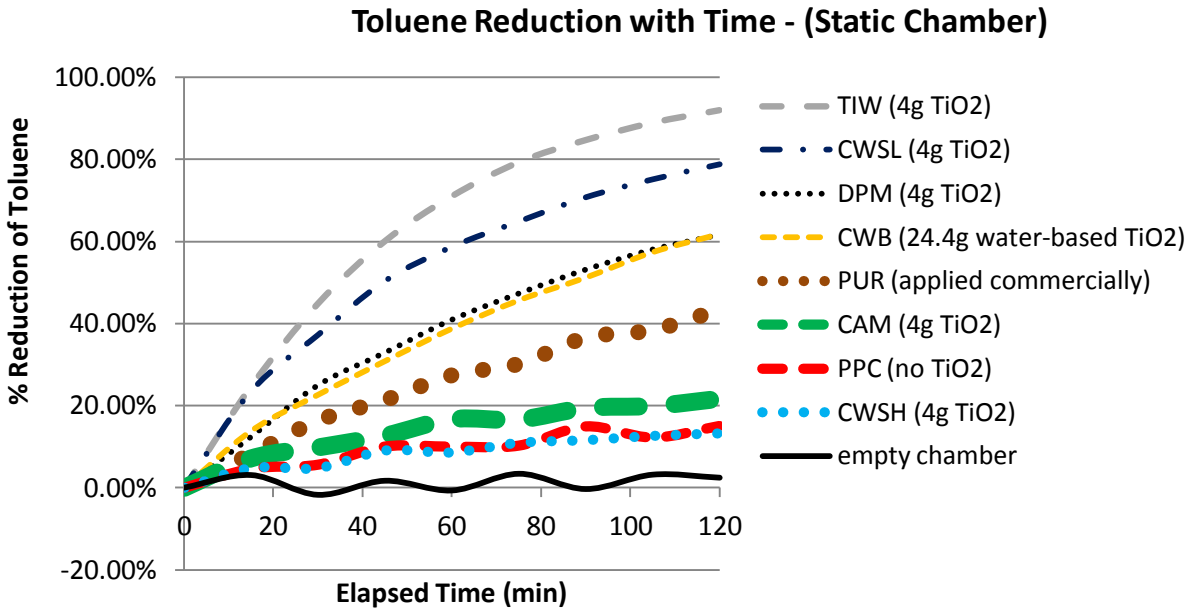

(a)

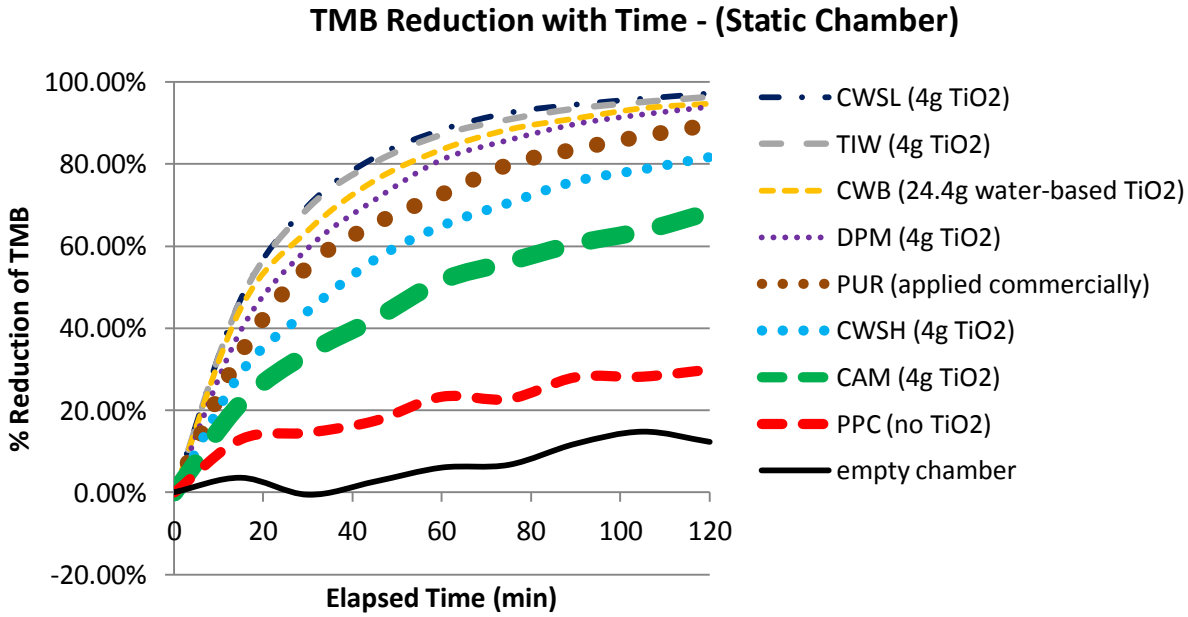

(b)

Figure 4.6: Static chamber results for final-evaluation samples tested with (a) Toluene and (b) TMB

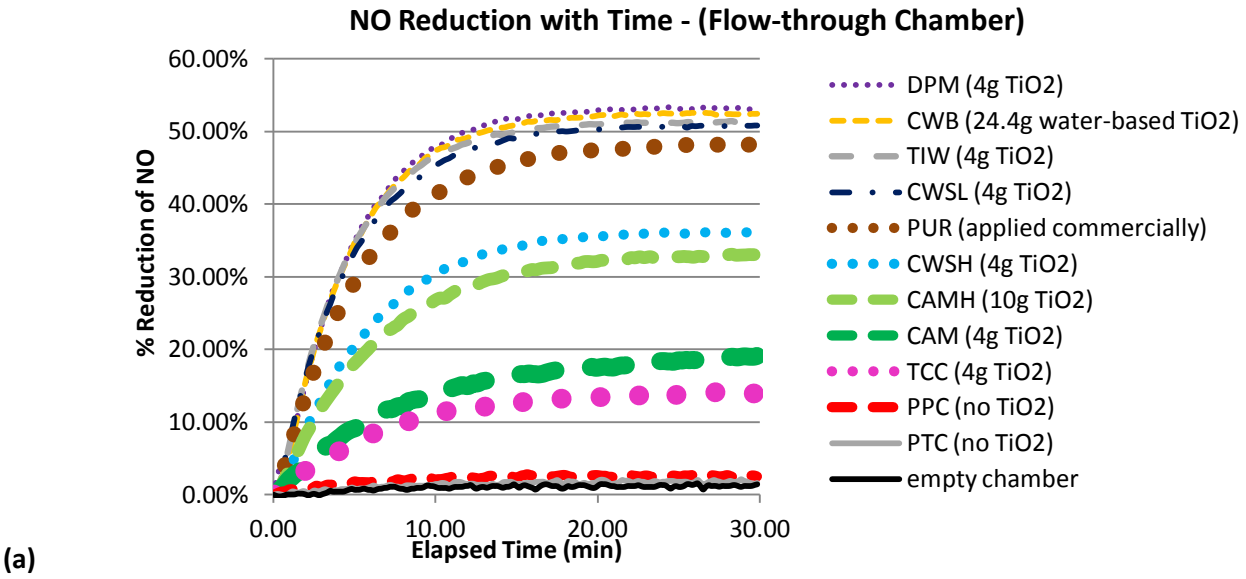

(a)

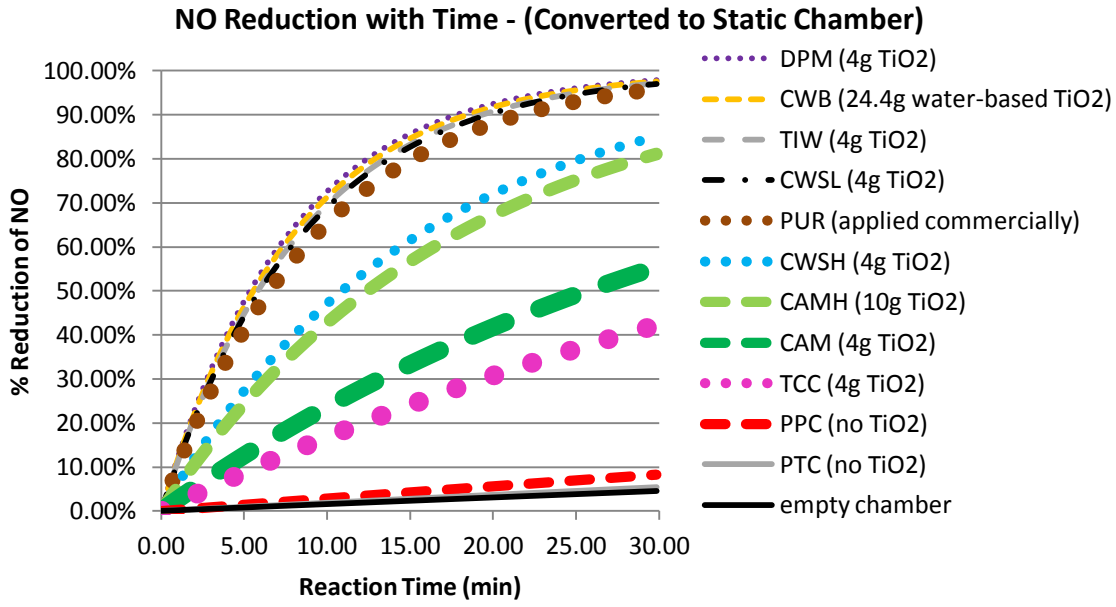

(b)

Figure 4.7: Results for NO reduction for final-evaluation samples with (a) flow-through chamber data and (b) converted to static chamber data

When observing the removal of different pollutants due to photocatalytic TiO_2, NO reacted most effectively followed by TMB and then toluene. NO reduction reached over 95% for

a reaction time of less than half an hour for many cases. Toluene was reduced usually less than 60% for a 2 hour reaction time. All three pollutant types had an increasing curve trend for percent reduction with time. After performing nonlinear (intrinsically linear) regression analysis, the percent reduction of Toluene showed closer to a $\ln(time)$ relationship. The percent reductions in TMB and NO both showed closer to a $-inv(time)$ relationship. Figure 4.8a shows the ln(time) model fitted to the percent toluene reduction curves for three different sample types, TIW, DPM, and CWB. Figure 4.8b shows the –inv(time) model fitted to the TMB reduction curves for TIW, DPM, and CWB. Figure 4.8c shows the –inv(time) model fitted to the NO reduction curves for TIW, DPM, and CWB. As shown the proposed models fit the experiment curves well for most of the cases. It is recommended that future study could use the developed models to quantify the effectiveness of pollutant reduction for a specific treatment method.

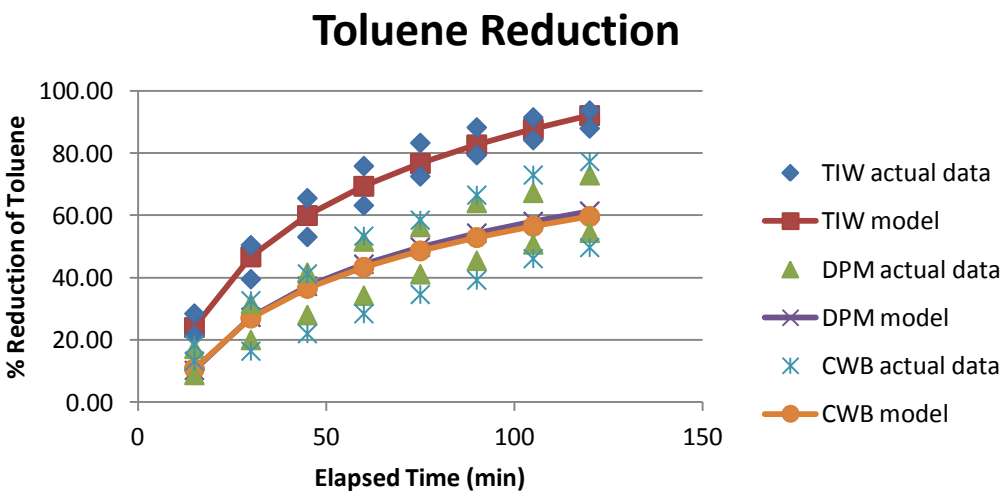

% Toluene Reduction with time :

TIW model : toluene % reduction = -64.6112 + 32.73361 * ln(time), $R^2 = 0.949$

DPM model : toluene % reduction = - 56.2786 + 24.57954 * ln(time), $R^2 = 0.808$

CWB model : toluene % reduction = - 52.8998 + 23.51582 * ln(time), $R^2 = 0.633$

(a) ***(Figure 4.8)***

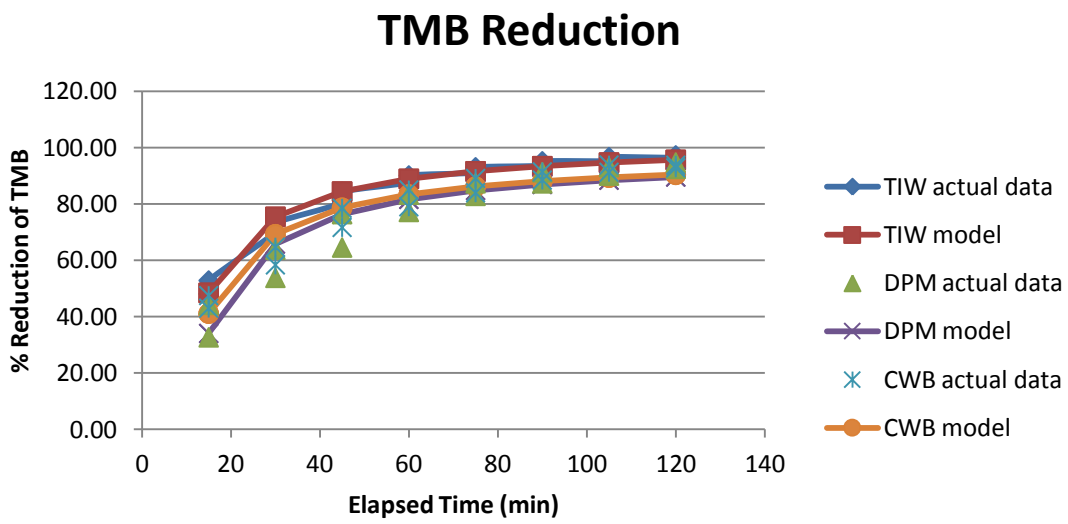

$$\%\,TMB\,Reduction\ with\ time:$$

$$TIW\ model: TMB\%\ reduction = 102.3625 - 808.822/(time), \quad R^2 = 0.976$$

$$DPM\ model: TMB\%\ reduction = 97.48225 - 951.572/(time), \quad R^2 = 0.906$$

$$CWB\ model: TMB\%\ reduction = 97.37691 - 844.174/(time), \quad R^2 = 0.923$$

(b) ***(Figure 4.8)***

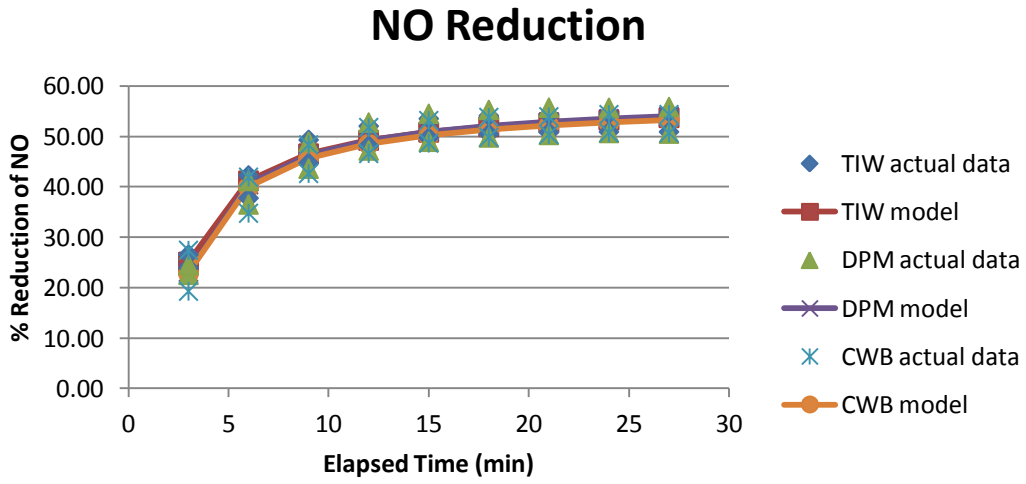

(part of Figure 4.8 c)

% NO Reduction with time:

TIW model: NO % reduction = 57.29257 - 96.6269/(time) $R^2 = 0.948$

DPM model: NO % reduction = 57.87231 - 104.437/(time) $R^2 = 0.927$

CWB model: NO % reduction = 56.99371 - 102.37/(time), $R^2 = 0.918$

(c) ***(the remaining part of Figure 4.8 c)***

Figure 4.8 Pollutant reduction models for TIW, DPM, and CWB samples: a) % toluene reduction with time, b) % TMB reduction with time, and c) % NO reduction with time

Several surface treatment methods showed significant pollutant reduction, among which CWB, DPM, TIW, CWSL, and PUR were the highest with over 89% for TMB reduction and over 95% for NO reduction (static). There was not one method that had the highest reduction in all pollutants simultaneously; some methods reacted better with certain pollutants than others. DPM showed the highest static NO reduction, CWSL showed the highest static TMB reduction, and TIW showed the highest static toluene reduction. Further testing with TIW was stopped, as the coating would not stick well to the surface and would come off with the touch of a hand.

When pervious concrete was compared to traditional concrete, the pervious concrete showed higher static NO reductions, whether the sample had TiO_2 coating on it or not. When samples had a cement-slurry coating of 5% TiO_2, the pervious concrete (CWSH) showed 85.0% static NO reduction, while traditional concrete (TCC) showed 42.2% static NO reduction. Plain pervious concrete (PPC) showed a static NO reduction of 8.3%, while plain traditional concrete (PTC) showed a static NO reduction of 5.4%. Part of the reason for the pollutant reduction seen with these samples could be attributed to photocatalytic compounds that may originally exist in the concrete such as zinc oxide (ZnO). Pervious concrete performed better than traditional

concrete most likely due to its high porosity and surface areas, resulting in increased photocatalytic effect under UV light.

4.2.1.3 Optimization of DPM coating method

Because the driveway protector mix (DPM) treatment method showed promising results in reducing the pollutants in the environmental chamber and withstand weathering, four more samples with this method were prepared to compare the DPM's effectiveness at 5%, 10%, 15%, and 18% concentration of TiO_2. The original DPM that was first tested on the final-evaluation samples had 14.29% TiO_2. Figure 4.9 shows the results for the different DPM concentrations.

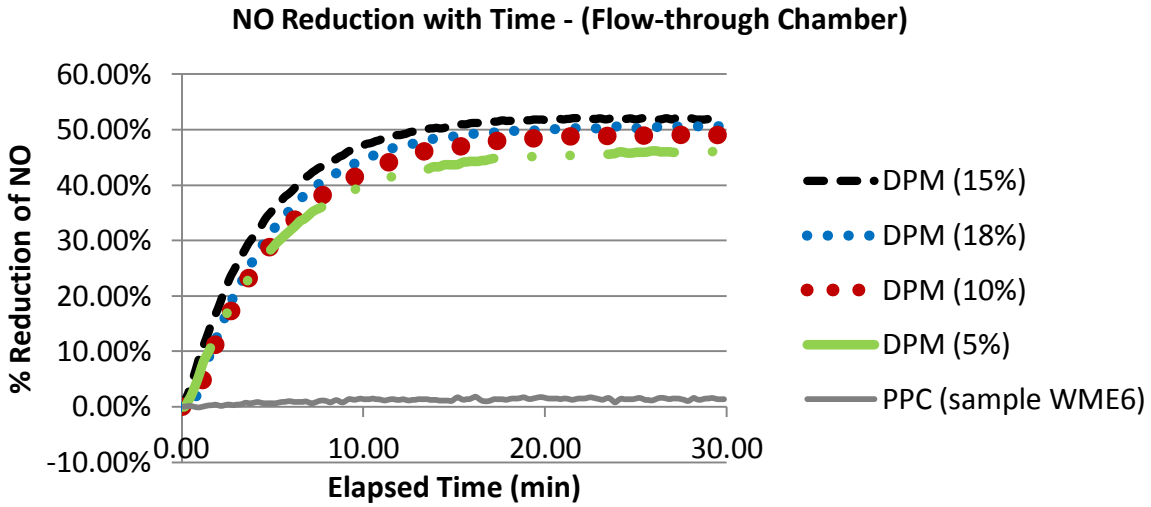

(a) *(Figure 4.9)*

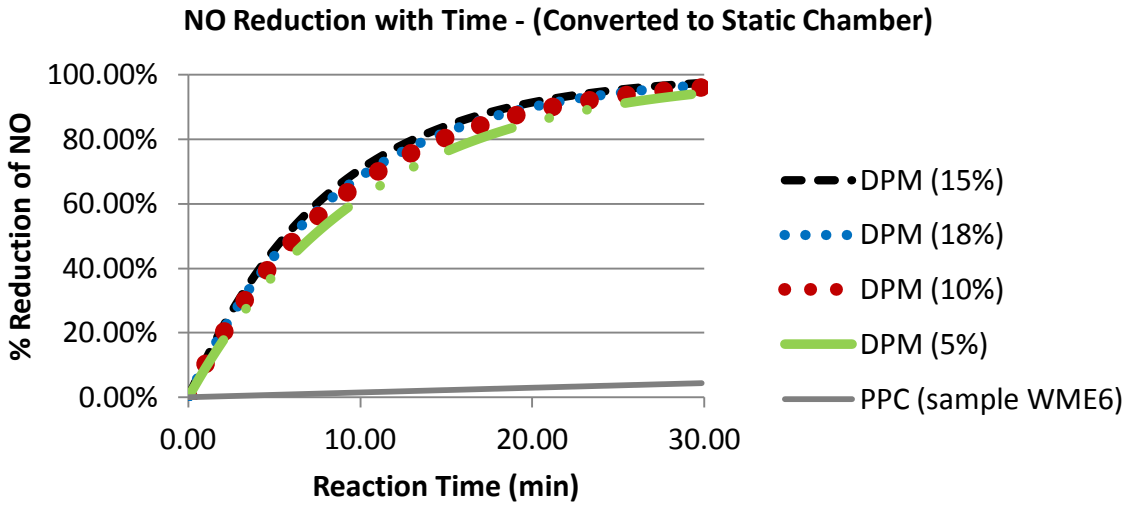

(b)

Figure 4.9: Results for NO reduction for DPM coatings on final-evaluation samples with (a) flow-through chamber data and (b) converted to static chamber data

The results for the different TiO_2 concentrations of DPM treatment were not too different, as they all produced between 46% and 53% NO flow-through reduction. This corresponds to between 94% and 98% NO reduction for a 30 minute reaction time. This shows that the DPM treatment could still be effective with a smaller amount of TiO_2 as low as 5% by weight of the driveway protector mix, which will save in material costs for the TiO_2.

4.3 SEM IMAGE ANALYSIS

Scanning Electron Microscopy (SEM) was used to determine the TiO_2 distribution at the surface. Two different scanning electron microscopes were used: the Hitachi S-570 (Figure 4.10) and the FEI 200F. Small segments of the pervious concrete materials with different surface treatment types were sampled from the pervious concrete specimens for viewing under the

SEMs. Each segmented specimen, less than ½ inch in diameter and less than ¼ inch in height, was adhered to a 12 mm diameter tab with carbon tape for placement inside the SEM. Specimens were coated with gold using a gold sputter coater so that the SEM could detect a clearer picture, as the high conductivity of gold produces high topographic contrast and resolution in the SEM.

Because both the TiO_2 and the concrete were light colored, and the particles in the concrete were similar in shape to the TiO_2 particles, it was often difficult to distinguish between the two. The rough texture of the concrete helped camouflage the TiO_2 particles. Another thing that may have contributed to this difficulty in TiO_2 identification was the thickness of the gold coating, which may have prevented the actual texture of the surface from showing. It would be easier to identify the TiO_2 by its white color against the darker gray concrete, but the SEM images are in grayscale, and the contrast/brightness of the image is mostly arbitrary, as it is manually adjusted by the user. Also, the specimens were coated with gold coating, which made the whole sample gold in appearance.

Figure 4.11 compares Hitachi SEM images of a) TiO_2 powder and b) cement powder at 1000 times magnification. Both powders appeared light colored, except the TiO_2 image showed up brighter, even when the contrast and brightness was adjusted to lower levels. The TiO_2 particles seemed finer, however, the particle size was not consistent for both TiO_2 and cement powders. Some of the TiO_2 particles formed into larger masses, and some of the cement particles were broken into smaller masses. The cement particles overall seemed more angular shaped than the ultra-fine TiO_2 particles.

Figure 4.10: Hitachi SEM used for viewing TiO_2 surface coatings

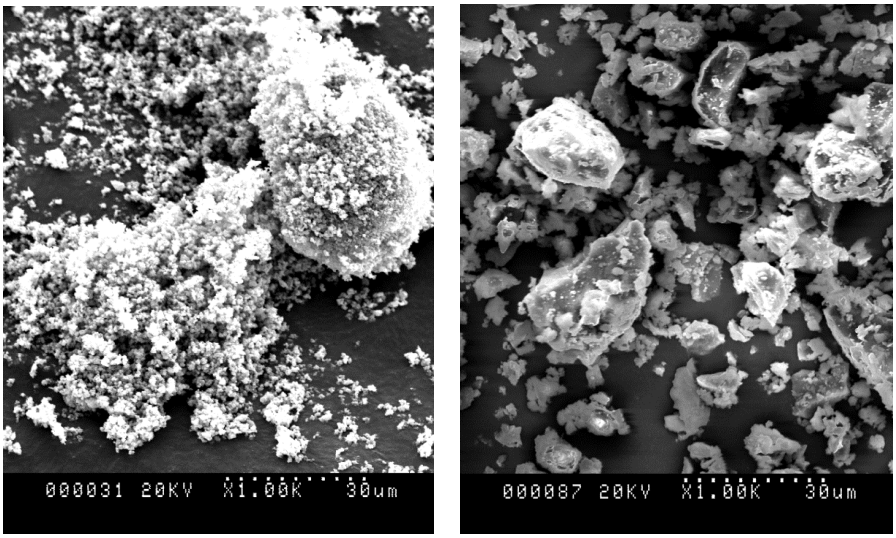

(a) **(b)**

Figure 4.11: Hitachi SEM images of a) TiO_2 powder alone and b) cement powder alone at 1000 times magnification

Figure 4.12 compares Hitachi SEM images of a) plain pervious concrete with no TiO_2 treatment (PPC) and b) pervious concrete with TiO_2 sprinkled on it when it was fresh (SFC, sample WMS4) at 1000 times magnification. Both images show a spiky/furry texture, with more furry texture on the plain pervious concrete specimen than on the TiO_2 treated specimen, but there is no obvious indication of TiO_2 particles in either image. Both images have an almost

uniform color and have no areas where the color is significantly brighter or darker than the rest of the area. The TiO_2 particles may not be seen in Figure 4.8b because the texture of the pervious concrete alone is very rough in comparison to the small ultra-fine TiO_2 particles.

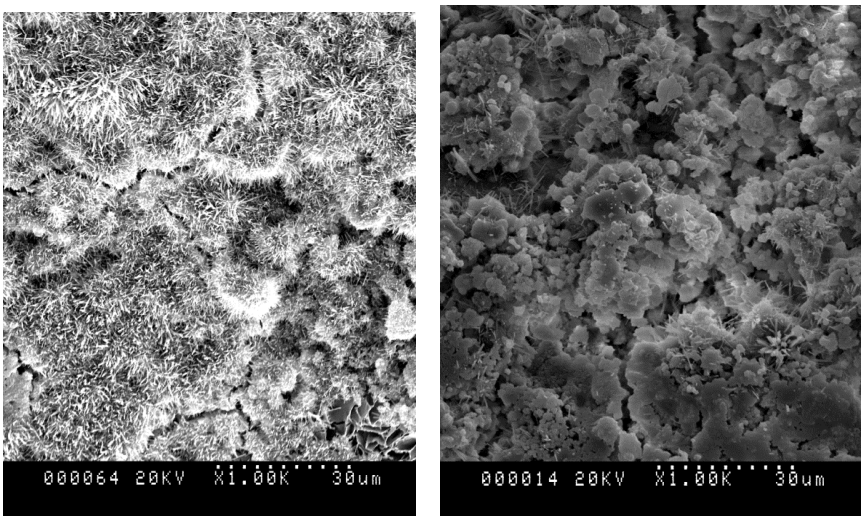

(a) **(b)**

Figure 4.12: Hitachi SEM image of a) plain pervious concrete with no TiO_2 (PPC) and b) TiO_2 sprinkled on pervious concrete when it was fresh (SFC, sample WMS4) at 1000 times magnification

Figure 4.13 compares Hitachi SEM images of a) pervious concrete treated with cement-water slurry (CWSH, sample WMA9) and b) pervious concrete treated with driveway protector mix (DPM, sample WMC7) at 2000 times magnification. Unlike Figure 4.12, the images a and b in Figure 4.13 show some particles with higher contrast (whiter color) on the top of the surface, which could possibly be the TiO_2 particles exposed on the top of the treatment layer. Visible cracks were seen in the cement-water slurry layer, while no large cracks were seen in the driveway protector mix layer at the same magnitude. With the exception of the lighter-colored particles sitting on the top of the surface, the texture of the cement-water slurry layer was

relatively smooth compared to the furry texture seen in the plain and TiO_2-sprinkled pervious concrete specimens in Figure 4.12. The driveway protector mix showed mostly small particles, similar in shape to the TiO_2 particles seen in Figure 4.11a. These particles seem more abundant and evenly distributed over the top of the surface of the driveway protector mix, which could contribute to its high performance in removing air pollutants in section 4.2. Even though CWSH had the same amount of TiO_2 on it, DPM had the TiO_2 spread out more evenly and was mostly exposed to the surface. Not all of the TiO_2 particles in CWSH were exposed on the top surface. Due to the high ratio of cement in CWSH, it is expected that the cement would thickly coat over the TiO_2. This is why the CWSL coating was made with a lower cement ratio, and the pollutant-removal effectiveness was higher for CWSL than for CWSH as expected.

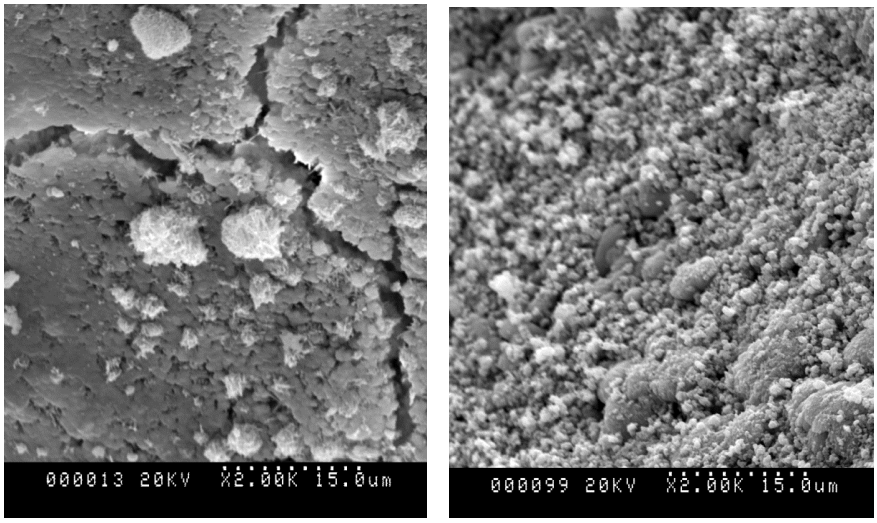

(a) **(b)**

Figure 4.13: Hitachi SEM image of a) pervious concrete treated with cement-water slurry (CWSH, sample WMA9) and b) pervious concrete treated with driveway protector mix (DPM, sample WMC7) at 2000 times magnification

Figure 4.14 shows an FEI SEM image of pervious concrete treated with commercial water-based TiO_2 (CWB) at 10,000 times magnification. At this strong magnification, white particles were highly evident and resembled the TiO_2 particles seen in Figure 4.11a. The surrounding surface that the white particles rested on top was relatively smooth with small cracks. The surface did not have the furry texture that was seen with the plain and TiO_2-sprinkled pervious concrete specimens in Figure 4.12. As with the driveway protector mix, exposure of the TiO_2 particles on the surface of the commercial water-based TiO_2 layer could contribute to its high performance in removing air pollutants in section 4.2.

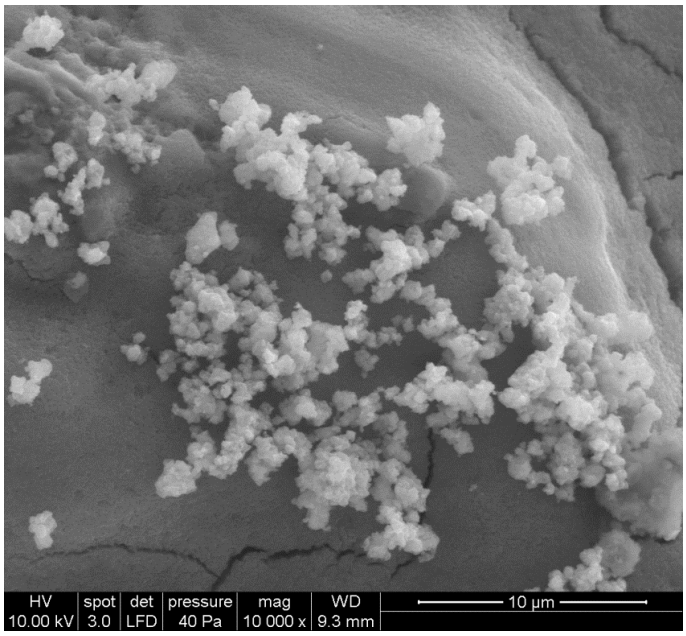

Figure 4.14: FEI SEM image of pervious concrete treated with commercial water-based TiO_2 (CWB) at 10,000 times magnification

4.4 DURABILITY

4.4.1 In-Lab Durability

The two sets of the final-evaluation samples with the treatments, CWB, CWSH, CWSL, DPM, PUR, CAM, CAMH, and PPC, were made for two different types of durability tests. One of those sets was used for evaluating durability in a freeze-thaw environment (an in-lab test). The resistances of the TiO_2 coatings were evaluated against exposure to deicing chemicals using a modified version of ASTM Standard C672 (2003). Since the samples were pervious concrete, it was impossible to maintain a puddle of solution on the surface, as the ASTM standard C672 required. A more realistic drained approach was followed, similar to the test method suggested by another pervious concrete study (Cutler et al., 2010). Samples were placed in containers with three $\frac{1}{10}$ inch (2.54 mm) holes drilled into the bottom. A solution with 9% by mass of calcium chloride was poured onto the surfaces of each sample until the sample was covered with solution 6 - 12 mm above the surface. While placed inside a 14 ft^3 (0.392 m^3) freeze-thaw chamber, solutions were allowed to slowly drain into separate containers at 70 ± 30 mL/min. One cycle in the freeze-thaw chamber consisted of two hours at -18°C and 2 hours at 10°C. The deicing solution was changed every 12 cycles, and the experiment was performed for 36 cycles. The amount of NO reduction by each sample was tested in the environmental chamber after 0 cycles, 12 cycles, and 36 cycles. The results are shown in Figure 4.15 with static chamber data.

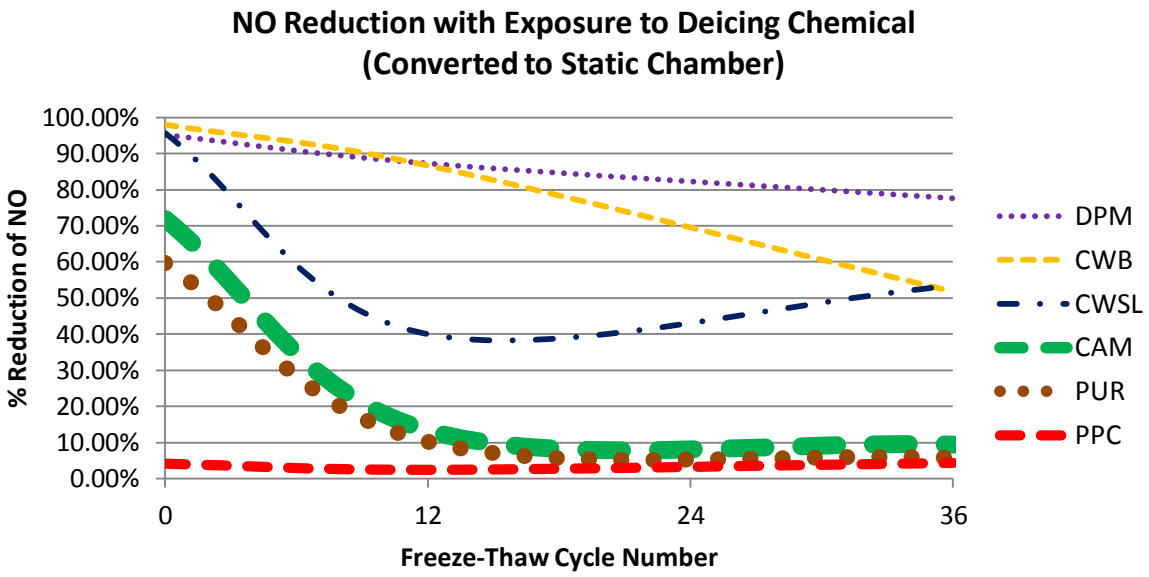

Figure 4.15: Results for NO reduction after 0, 12, and 36 freeze-thaw cycles and exposure to deicing chemical

By the end of 36 cycles, most pervious concrete specimens were heavily damaged, indicating low resistance to calcium chloride solution. Out of the samples that remained, DPM had the highest resistance to the deicing agent and freeze-thaw cycles, with a 95.10% static NO reduction before any testing and a 77.68% static NO reduction after 36 cycles. Other sample types ended with below 54% static NO reduction after 36 cycles. Note that these results are based on testing one sample per sample type. No repetition test was conducted because it is a time consuming test, and the consistency with each type was seen during the initial chamber testing

4.4.2 Outside Durability

To observe the effects of weathering on the surface coatings, the other set of final-evaluation samples with the treatments, CWB, CWSH, CWSL, DPM, PUR, CAM, CAMH, and

PPC, was placed outside to have actual weather exposure (an outside durability test). Figure 4.16 shows the samples the first day they were placed outside for weathering. Figure 4.17 shows the temperature range and precipitation the samples were exposed to during their time period sitting outside. The samples sat outside for the entire summer in Pullman, Washington from May 13, 2011 to September 21, 2011. Table 4.3 and Figure 4.18 summarize and graphically show the NO converted-to-static chamber results respectively for the samples before weathering, after 3 months of weathering, after 4 months of weathering, and after they had been washed with a soft bristle brush and water after 4 months of weathering.

Figure 4.16: Samples outside for weathering

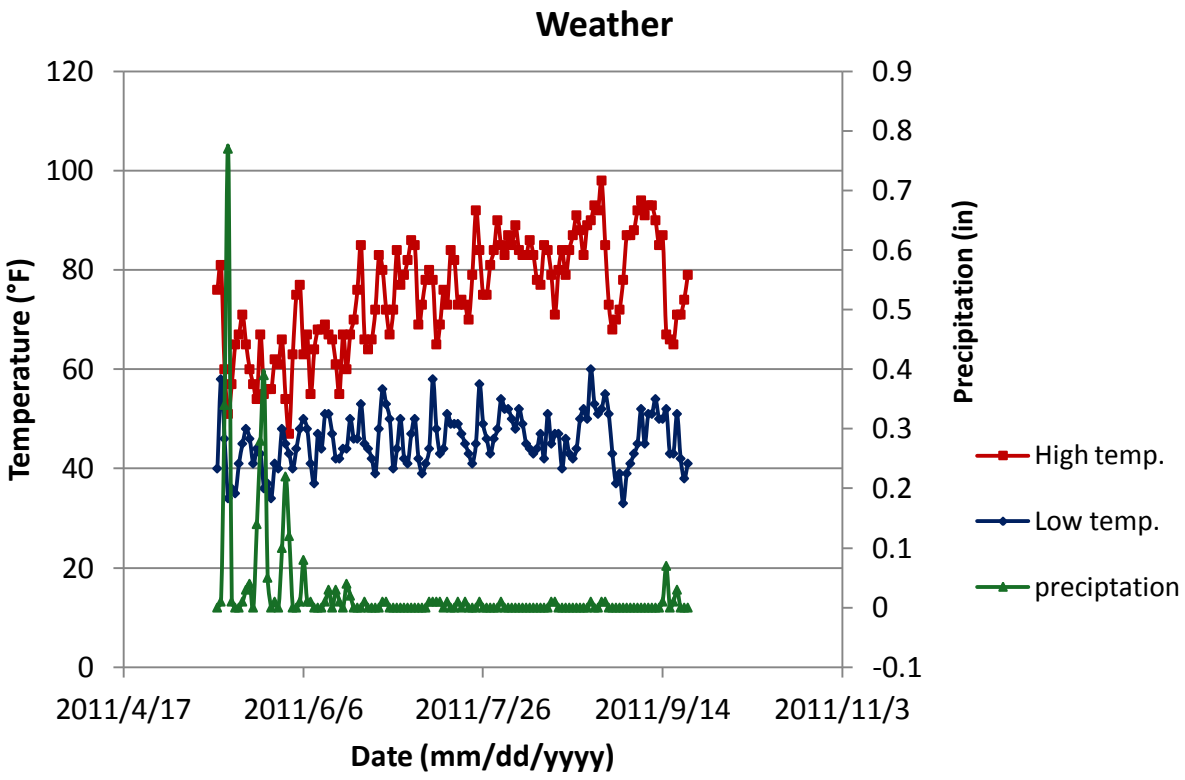

Figure 4.17: The temperature and precipitation during the time when the samples were being weathered outside. (Weather data from: www.wunderground.com)

Table 4.3: Summary Table of Results for NO reduction after 0, 3, and 4 months of weathering, and after washing the samples after 4 months of weathering

Surface Treatment	Converted Static Chamber (29.83min) Total %NO Reduction			
	Before Weathering	After 3 Months Weathering	After 4 Months Weathering	After 4 Months Weathering (after washing)
CWB	97.04%	70.30%	55.04%	89.47%
CWSH	85.04%	16.00%	10.03%	13.14%
CWSL	97.09%	78.45%	63.50%	79.46%
DPM	96.91%	88.13%	73.81%	91.80%
PUR	94.44%	3.82%	5.66%	6.98%
CAM	49.13%	6.87%	4.08%	5.62%
CAMH	79.25%	18.00%	10.95%	10.94%
PPC	8.78%	1.23%	2.86%	2.74%

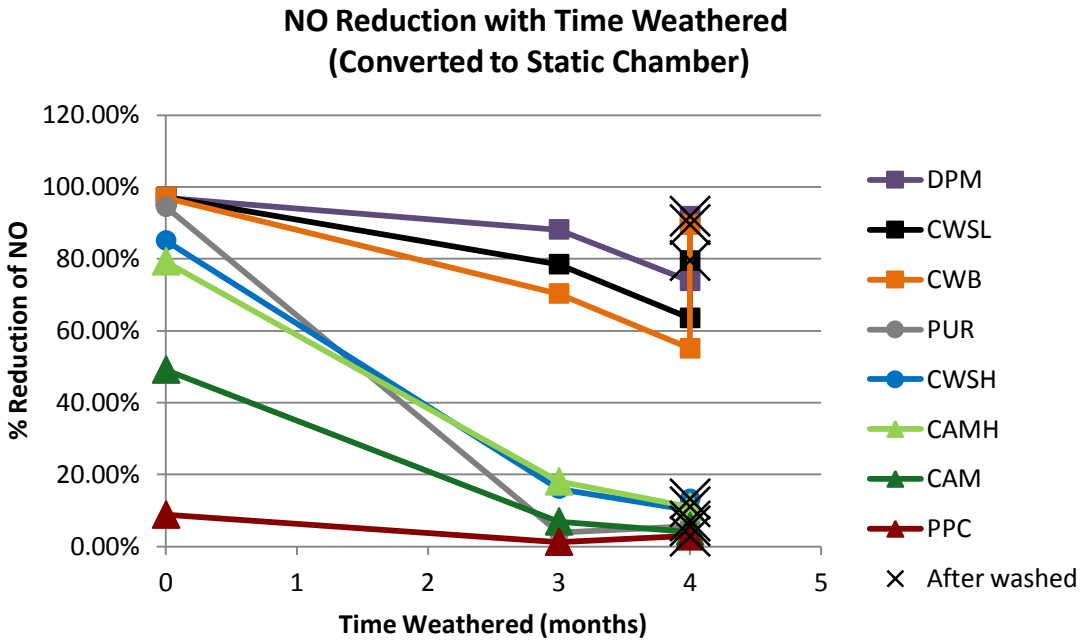

Figure 4.18: Graphical results for NO reduction after 0, 3, and 4 months of weathering, and after washing the samples after 4 months of weathering

All samples showed significant decrease in their NO % reductions after weathering. Most samples showed improvement after washing, but none of them reduced NO at the level they once had before weathering. DPM had the highest resistance to weathering, with a 96.91% static NO reduction before weathering and a 73.81% static NO reduction after 4 months weathering. The CWB and CWSL treatments also resisted fairly well. PUR started with a high static NO reduction of 94.44% before weathering and ended with a low static NO reduction of 5.66% after 4 months weathering. Note that these results are based on testing one sample per sample type. No repetition test was conducted because it is a time consuming test, and the consistency with each type was seen during the initial chamber testing

4.5 FIELD TRIAL

Two of the most effective coatings, the commercial water-based TiO_2 (CWB) and the driveway protector mix (DPM), were painted on sections of an actual newly paved pervious concrete sidewalk located between two sports playfields in Pullman, Washington for scaling observation (figure 4.19a). The sidewalk endured the same type of weathering at the same time of year as the weathering samples in section 4.4.2. Both coatings were painted on two different 2 ft. by 2 ft. areas each for observation. The set-up is shown in figure 4.19b, with coating A as the DPM coating and coating B as the CWB coating. As shown in figure 4.19a, the DPM coating adds an obvious white color to the pavement, while the CWB coating turns the pavement a slightly lighter gray. Figure 4.20 shows the coatings on the pervious concrete with time, with the weather condition and date on which the photo was taken indicated on each image.

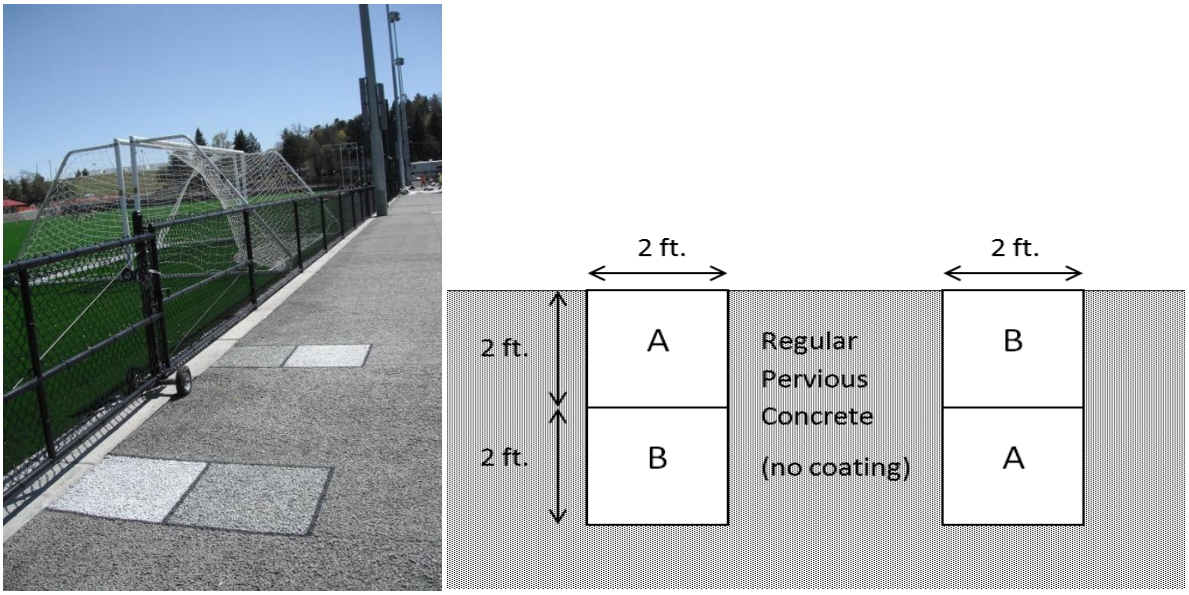

Figure 4.19: (a) Field coatings on the pervious concrete sidewalk a) on the first day of placement, and b) a diagram showing the placement of each coating, with coating A: driveway protector mix (DPM) and coating B: commercial water-based TiO_2 (CWB)

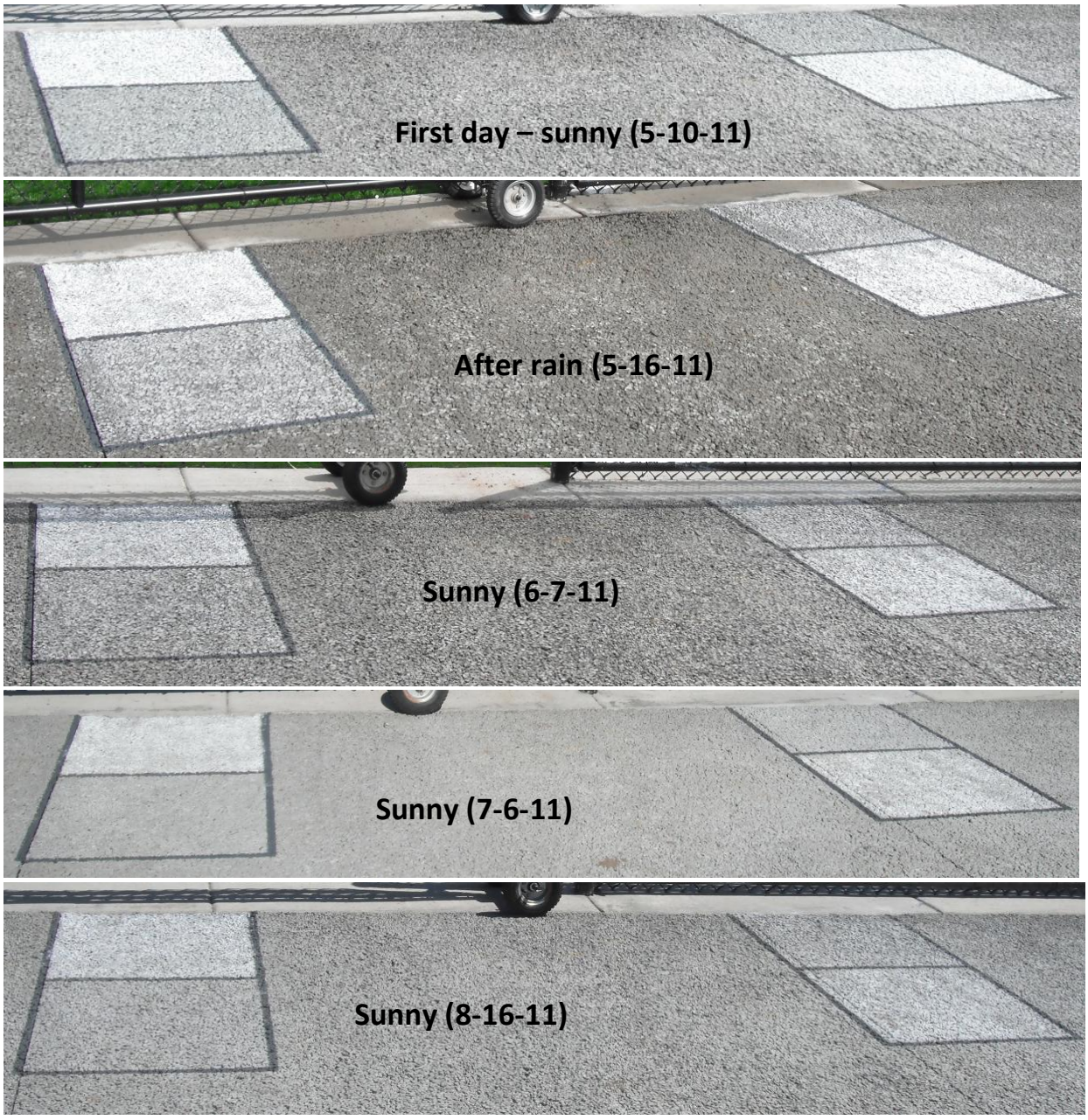

Figure 4.20: Field coatings on the pervious concrete with time (weather condition and date indicated on each image), starting the top-most image as the first day on May 10, 2011 to the bottom-most image on August 16, 2011

With time, both coatings had faded in color. Scaling conditions did not start yet, as the concrete had only been exposed to summer weather thus far. After 3 months, the appearance of

the CWB coating was not as distinguishable from the regular un-coated pervious concrete as it originally was. The DPM coating, though slightly more faded than it originally was, was still a white color. The white color of the DPM coating communicates to the observer that the coating is still there and still working to effectively remove pollutants, whereas with the CWB coating, it is unknown whether the coating has come off due to abrasive forces or if it's even working still. If these coatings were applied in the field, the DPM coating could be re-applied as a maintenance fulfillment whenever it was obvious that the color had worn away.

4.6 COST ANALYSIS

An approximate estimate for the material cost of each treatment method that was used in the final-evaluation sample sets for durability testing (CWB, CWSH, CWSL, DPM, PUR, CAM, and CAMH) is shown in Table 4.4. This is based on the rates without bulk-discounts or labor costs. The rate for commercial water-based TiO_2 (S5-300B) and ultra-fine TiO_2 (PC105) are each about $20.40 per kg. The PURETI coating application is about $0.10 per ft^2. The driveway protector (Seal-Krete) is about $18.18 per gallon. Type I Portland cement is about $12 per 42 kg. Small pea-rock aggregates are about $39 per ton. A column of the overall effectiveness of toluene, TMB, and NO reduction, as well as the decrease in infiltration rate for each coating method is also shown in Table 4.4 to provide an overview of the cost-effectiveness of each application.

Table 4.4: Material Cost for Each Coating Type

Coating type	MATERIAL COST		OBSERVED POLLUTANT REDUCTION			
	total material cost ($/ft^2)	total material cost ($/m^2)	Static Chamber (120 min) total % toluene reduction	Static Chamber (120 min) total % TMB reduction	Converted Static Chamber (29.83 min) Total % NO reduction	% Decrease in infiltration rate
commercial water-based TiO_2 (CWB)	0.9955	10.70	61.86±14.06%	94.64±1.85%	97.59%	20.60%
cement-water slurry (CWSH)	0.1860	2.00	13.23±1.62%	81.65±1.50%	85.04%	58.29%
driveway protector mix (DPM)	0.3876	4.17	61.65±10.77%	93.87±1.09%	97.92%	30.49%
Pureti (PUR)	0.1000	1.08	43.42±1.79%	89.50±4.05%	95.79%	11.92%
cement-water slurry low (CWSL)	0.1655	1.78	78.82±9.22%	97.26±0.63%	96.94%	51.50%
cement/aggregate mix (CAM)	0.3045	3.27	21.62±4.30%	68.28±5.99%	55.35%	3.85%
cement/aggregate mix high (CAMH)	0.3030	3.26	-	-	81.03%	-3.49%

- *This data is unavailable*

Based on the estimation in table 4.4, the cost to apply TiO_2 as a pavement surface treatment could vary widely, depending on what coating method is selected. Prices will range from the CWB method being the most expensive at $10.70 per m^2 to the PUR method being the least costly at $1.08 per m^2. It could also vary depending on how much area it would be applied onto. A large extensive area would receive bulk discounts on the materials compared to the

smaller samples used in this project for laboratory testing. Overall, the cost for TiO_2 application is relatively affordable.

CHAPTER FIVE

CONCLUSIONS AND FUTURE WORK

Because pavement has large surface area that is in contact with polluted air, treating pavements with TiO_2 could reduce harmful emissions at street level and benefit a cleaner living environment for the public. Unlike traditional non-pervious pavements, the high porosity and surface roughness of pervious concrete pavement allow more TiO_2 particles to have direct contact with UV lights and thus improve removal efficiency. The open pore structure of pervious concrete might also protect TiO_2 particles from traffic loading and environmental weathering. In addition to being a sustainable transportation facility for stormwater runoff management, pervious concrete pavement, when coated with TiO_2 and widely implemented in urban roads and highway shoulders, may result in improved air quality and thus a multi-phase cleaner transportation environment for future generations.

Of the different pollutants tested for photocatalytic reduction in this study, NO typically reacted most effectively followed by TMB and toluene. The highest reductions in pollutants were seen with the driveway protector mix (DPM), the commercial water-based TiO_2 (CWB), the TiO_2 in water (TIW), the low cement-water slurry (CWSL), and the PURETI coating (PUR), each showing over 95% static NO reduction and over 89% static TMB reduction. Of these five, PUR had the lowest effect on reducing the infiltration rate of the pervious concrete, with an 11.92% reduction in infiltration rate after the surface treatment. DPM had the highest resistance against the deicing chemical and freeze-thaw testing, maintaining a 77.68% static NO reduction after 36 freeze-thaw cycles. DPM also had the highest resistance against weathering, maintaining a 73.81% static NO reduction after 4 months of weathering and a 91.80% static NO reduction

after washing the samples after 4 months of weathering. When coated on an actual pervious concrete sidewalk outside, the DPM was more visually obvious than CWB that the TiO_2 coating did not wear completely off within 4 months of exposure to natural weathering. When pervious concrete was compared to traditional concrete, the pervious concrete showed higher static NO reductions, whether the sample had TiO_2 coating on it or not.

When DPM coatings were compared at different TiO_2 concentrations (5%, 10%, 15%, and 18% TiO_2), all four concentrations had similar results for NO reduction, maintaining between 94% and 98% static NO % reduction. This shows that the DPM coating can still work well with lower amounts of TiO_2; in other words, a higher concentration of TiO_2 is not needed for DPM coating. Image analysis under the scanning electron microscope (SEM) revealed lighter-colored particles, which resembled TiO_2, to be more abundant and uniformly distributed on the surface of the DPM coating. Exposure of the TiO_2 particles on the surface, as seen in the SEM for DPM, CWSH (high cement-water slurry), and CWB layers, could contribute to high performance in removing air pollutants in section 4.2.

Each coating type in this study could be useful for different purposes. For example, because the DPM maintained its high photocatalytic activity after exposure to deicing chemical and freeze-thaw cycles, this type of coating could be used in a highly abrasive environment, like on the shoulders of a highway or on busy sidewalks adjacent to a road. The CWB could be used for aesthetic reasons, where the white color of the DPM is not desired; the CWB is a transparent coating. The white color of the TiO_2 particles seen in the DPM coating could potentially be used as pavement marking materials, at the same time achieving air purification effect. The CAM and CAMH coating, TiO_2 mixed into thin pervious concrete overlay, could be used as a pavement maintenance technique to address minor surface raveling and cracking distresses at the same

time produce photocatalytic effect. The PUR is a cost-effective light coating, which is suitable for wide low traffic area where the surface abrasion is low.

Because the TiO_2 application on pavements for photocatalytic oxidation is still a relatively new area, more research should be conducted prior to application in the field. The coatings still need be tested for resistance in the fall, winter, and spring months, as well as be tested for resistance to vehicle abrasion. More in-depth research should also be conducted to investigate the overall effect of the photocatalytic reaction and if any, harmful chemical compound could be produced during such reaction to adversely affect the environment and human health before the wide application of the photocatalytic materials for improved environment benefit.

REFERENCES

ASTM Standard C672/C672M (2003). "Standard Test Method for Scaling Resistance of Concrete Surfaces Exposed to Deicing Chemicals," ASTM International, West Conshohocken, PA, DOI: 10.1520/C0672_C0672M-03, www.astm.org.

ASTM Standard C1701/C1701M (2009). "Standard Test Method for Infiltration Rate of In Place Pervious Concrete," ASTM International, West Conshohocken, PA, DOI: 10.1520/C1701_C1701M-09, www.astm.org.

Berthelot, A. (2010). Concrete Steps: LSU Professor to Lay Pollution-Cleaning Pavement on Campus and Aster Street Dec. 13 – First time in United States that air purifying concrete and asphalt pavement have been laid. *Louisiana State University*. Retrieved January 2, 2011, from http://www.lsu.edu/ur/ocur/lsunews/MediaCenter/News/2010/12/item22709.html

Bolt, J. R., Zhuge, Y., & Bullen, F. (2011). Photocatalytic construction materials: An overview of recent developments and their application to permeable concrete. *Incorporating Sustainable Practice in Mechanics of Structures and Materials,* pp. 821-825.

Brown, D. (2003). Pervious Concrete Pavement: A Win-Win System. *Concrete Technology Today*, Portland Cement Association (PCA), CT032, Vol. 24, No. 2.

Chai-Mei Yu, J. (2003). *Deactivation and Regeneration of Environmentally Exposed Titanium Dioxidde (TiO_2) Based Products*. Testing Report Departmental Order Ref. No. E183413, Environmental Protection Department (EPD), HKSAR.

Chen, D. H., Li, K., & Yuan, R. (2007). Photocatalytic Coating on Road Pavements/Structures for NOx Abatement. (Annual Project Report, Texas Air Research Center, Lamar University, 2007). *Houston Advanced Research Center and Office of Air Quality Planning and Standards, U.S. Environmental Protection Agency*. Research Triangle Park, NC.

Chen, M., & Liu, Y. (2010). NOx removal from vehicle emissions by functionality surface of asphalt road. *Journal of Hazardous Materials*, Vol. 174, pp. 375-379.

Cho, I., Kim, Y., Yang, J., Lee, N., & Lee, S. (2006). Solar-Chemical Treatment of Groundwater Contaminated with Petroleum at Gas Station Sites: Ex Situ Remediation Using Solar/TiO_2 Photocatalysis and Solar Photo-Fenton. *Journal of Environmental Science and Health Part A*, Vol. 41, pp. 457-473.

Chusid, M. (2006). *Photocatalysts keep concrete clean and depollute the air we breathe*. Precast Solutions. http://www.solutions.precast.org/precast-concrete-depollution-and-photocatalysis-case-study. Accessed Jan. 2, 2011.

Cutler, H. E., Wang, K., Schaefer, V. R., & Kevern, J. T. (2010). Resistance of Portland Cement Pervious Concrete to Deicing Chemicals. In Transportation Research Record: Journal of the Transportation Research Board, No. 2164, Transportation Research Board of the National Academies, Washington, D.C., pp. 98-104.

Dylla, H., Hassan, M. M., Mohammad, L. N., Rupnow, T., & Wright, E. (2010). Evaluation of the Environmental Effectiveness of Titanium Dioxide Photocatalyst Coating for Concrete Pavement. *Transportation Research Board 89th Annual Meeting* (Publication No. 10-0963). Washington, D.C.

Fernandez-Rodriguez, H., Alonso, E., & Jose Cocero, M. (2009). *Synthesis of Doped Nanoparticles in Supercritical CO_2*. International Society for Advancement of Supercritical Fluids. *9th International Symposium on Supercritical Fluids*. http://www.isasf.net/fileadmin/files/Docs/Arcachon/posters/p113-CO65%20alnso%209thMeeting_full_Alonso_Valladolid.pdf. Accessed March 7, 2011.

Frazer, L. (2001). Titanium Dioxide: Environmental White Knight? *Environmental Health Perspectives*, 109(4) A174-A177.

Ghafoori, N., & Dutta, S. (1995). Building and Nonpavement Applications of No-Fines Concrete. *Journal of Materials in Civil Engineering*, 7(4), 286-289.

Haselbach, L. (2009). Pervious Concrete and Mitigation of the Urban Heat Island Effect. Presented at 88th Annual Meeting of the Transportation Research Board, Washington, D.C.

Hashimoto, K., Irie, H., & Fujishima, A. (2005). TiO_2 Photocatalysis: A Historical Overview and Future Prospects. *Japanese Journal of Applied Physics*, Vol. 44, No. 12, pp. 8269-8285.

Hassan, M. M., Dylla, H., Mohammad, L. N., & Rupnow, T. (2010). Effect of Application Methods on the Effectiveness of Titanium Dioxide as a Photocatalyst Compound to Concrete Pavement. Presented at 89th Annual Meeting of the Transportation Research Board, Washington, D.C.

Hassan, M., Mohammad, L. N., Dylla, H., Cooper, A. M., & Asadi, S. (2011). A Breakthrough Concept in the Preparation of Highly-Sustainable Photocatalytic Warm Asphalt Mixtures. Presented at 2011 NSF Engineering Research and Innovation Conference, Atlanta, Georgia.

Hong, X., Wang, Z., Cai, W., Lu, F., Zhang, J., Yang, Y., Ma, N., & Liu, Y. (2005). Visible-Light-Activated Nanoparticle Photocatalyst of Iodine-Doped Titanium Dioxide. *Chem. Mater.*, Vol. 17, No. 6, pp. 1548-1552.

Inspection and Maintenance. (n.d.). *Pervious Pavement*. Retrieved October 17, 2010, from http://www.perviouspavement.org/inspection%20and%20maintenance.htm

Katzman, L. (2006). Building Toward a Cleaner Environment: A New Role for an Existing Product, TiO2. *Sasaki Associates Inc*. Retrieved January 2, 2011, from http://ideas.sasaki.com/files/attachments/user370/cleaner%20environment.pdf

Li, Z. (2011). Development and Application of Eco-Friendly Concrete. *Advanced Materials Research*. Vols. 250-253, pp. 3827-3836

Montes, F., & Haselbach, L. (2006). Measuring Hydraulic Conductivity in Pervious Concrete. *Environmental Engineering Science*, Vol. 23, No. 6, pp. 960-969.

Montes, F., Valavala, S., & Haselbach, L. (2005). A New Test Method for Porosity Measurements of Portland Cement Pervious Concrete. *Journal of ASTM International*, Vol. 2, No. 1.

Morales, A. (2011). London Exceeds Europe's Annual Pollution Goal Four Months Into Year. *Bloomberg*. http://www.bloomberg.com/news/2011-04-21/london-exceeds-europe-s-annual-pollution-goal-four-months-into-year.html. Accessed June 1, 2011.

Moussiopoulos, N., Barmpas, F., & Ossanlis, I. (2007). Numerical Study for the Potential Abatement of Air Pollution with the use of Photocatalytic Façade Covering Materials in London. Presented at 10th International Conference on Environmental Science and Technology, Kos Island, Greece.

New kind of cement absorbs pollution: An Italian company has begun marketing a cement that is capable of absorbing pollution from vehicles. (2006). *United Press International: Physorg*. Retrieved January 2, 2011, from http://www.physorg.com/news67012896.html

Obla, K. (2007). Pervious Concrete for Sustainable Development. *Recent Advances in Concrete Technology.* Washington DC.

Olek, J., Weiss, W. J., Neithalath, N., Marolf, A., Sell, E., & Thornton, W. D. (2003). *Development of Quiet and Durable Porous Portland Cement Concrete Paving Materials*. Publication SQDH 2003-5, Final Report, HL 2003-18, Purdue University.

Permeable or Pervious Pavers Cost Comparison (n.d.). *PaverSearch*. Retrieved October 17, 2010, from http://www.paversearch.com/permeable-pavers-costs.htm

Pervious Concrete: Mix Design and Materials (n.d.). *Torromeo Industries, Inc*. Retrieved October 10, 2011, from http://www.torromeo.com/Services/Mix-Design-and-Materials.html

Pervious Concrete Pavement: An Overview (n.d.). *Pervious Pavement.org*. Retrieved November 5, 2011, from http://www.perviouspavement.org/

Puzenat, E. (2009). Photocatalytic self-cleaning materials: Principles and impact on atmosphere. *The European Physical Journal Conferences*, Vol. 1, pp. 69-74.

Ramirez, A. M., Demeestere, K., De Belie, N., Mantyla, T., & Levanen, E. (2009), Titanium dioxide coated cementitious materials for air purifying purposes: Preparation, characterization and toluene removal potential. *Building and Environment*, Vol. 45, pp. 832-838.

Rocke, S., & Bowers, J. (2009). Use of pervious concrete is emerging in cold climates. *CE News*. Retrieved March 6, 2011 from http://www.cenews.com/print-magazinearticle-a_sustainable_pavement_alterna-6284.html

Shi, J., Chen, S., Wang, S., Wu, P., & Xu, G. (2009). Favorable recycling photocatalyst TiO_2/CFA: Effects of loading method on the structural property photocatalytic activity. *Molecular Catalysts*, Vol. 303, pp. 141-7.

Yang, J., & Jiang, G. (2003). Experimental study on properties or pervious concrete pavement materials. *Cement and Concrete Research*, Vol. 33, pp. 381-386.

APPENDIX

APPENDIX A

PROCEDURES OF PREPARING PERVIOUS CONCRETE SAMPLES

Below is the procedure followed for preparing all pervious concrete samples. Pervious concrete was mixed in a drum concrete mixer (figure A.1a) with the previously calculated material proportions, distributed into each sample mold with the previously calculated minimum/maximum mass range, and compacted to the previously determined volume with the concrete compactor form (figure A.1b).

Procedure:

1. Wet Mixer by using 2 lbs of water and 2 lbs of cement and then dump out into grate
2. Put the #8 aggregates in the bucket.
3. Put in all the aggregates, mix **1/2 minutes**.
4. Put in all cementitious materials and 1/2 of the water and mix **3 minutes**.
5. Put in the 1/2 remaining water (1/4 of original water) and mix **2 minutes**. Some mixture may stick on the bottom, knock it off.
6. Mix **3 minutes**. Knock the mixture (sticks on the mixer) off.
7. Rest **2 minutes** and do the "Ball test" (see below on how to do this test). If it could not form a ball, we should add more water in small increment then again mix **3 minutes** and rest **2 minutes** and then again do the "Ball test"… until the test is OK.
8. Mix **2 minutes**.
9. Put the concrete into the containers. Weigh the samples. Fill until at minimum mass-compacted.
10. Put special concrete form on top. Tamp with rubber mallet with light taps to line. (See Figure A.2 for a schematic on how to make and use the concrete form.)
11. Immediately cover with plastic covers
12. Cleaning up: dump all the extra concrete out onto the concrete scrap pile. Rinse out the equipment and tools over the grate.
13. Let the samples cure for 7 days
14. After 7 days remove covers as appropriate for each experiment condition.

Ball Test:

The ball test is performed to ensure that the pervious concrete samples were made to be "pervious," while still having a thick enough cement paste to strongly hold the aggregate structure together. If the paste is too thin (not enough water added), the concrete will be very pervious, but the structure will not hold well and will crumble easily. If the paste is too thick (too much water added), the structure will hold together strongly, but the concrete will not be pervious. The ball test is performed to ensure a balance between the two problems. This is why it

is carefully followed to add water at small increments at a time to prevent adding too much water and spoiling the mix.

A handful of pervious concrete formed into a ball should not crumble (Figure A.3a) nor should it lose its void structure (Figure A.3c) as the paste flows into the spaces between the aggregates. It should make a ball shape as shown in figure A.3b.

(a) **(b)**

Figure A.1: Making pervious concrete by a) mixing the pervious concrete mixture in a drum concrete mixer and b) compacting each specimen with a concrete compactor form

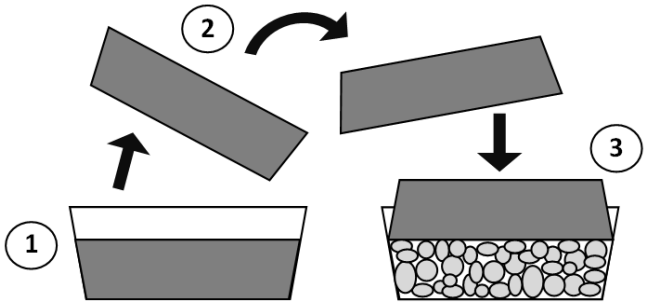

Figure A.2: A schematic diagram of making and using the compactor form: (1) compactor form is made in the same mold as the pervious concrete it will be compacting, (2) compactor form is taken out after it is cured and rotated to its top-side faced down on top of the pervious concrete, and (3) compactor form is ready to compact the pervious concrete

(a) (b) (c)

Figure A.3: The pervious concrete ball test when a) the ball crumbles (not enough water), b) the ball is good (just the right amount of water), and c) the ball loses its void structure (too much water) ("Pervious Concrete: Mix Design and Materials," n.d.)